



Internal Structure of Light Mesons Using Distribution Functions



Satyajit Puhan

working Under

Dr. Harleen Dahiya



Computational High Energy Physics Lab

Department of Physics ,

4th July, 2025

NIT J.

4th July, 2025

Asymptotic freedom



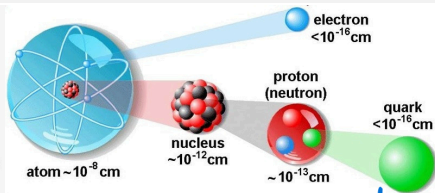
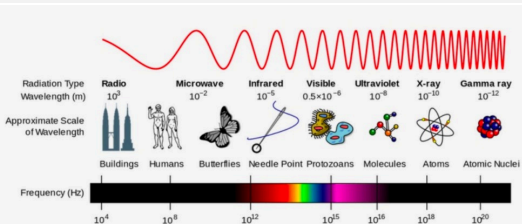
Confinement

No one has ever seen a free quark

- **Introduction**
- **Light-Front Dynamics**
- **Spin-0 and 1 TMDs, PDFs**
- **Spin-0 and 1 GPDs, FFs**
- **In-medium Properties**



Introduction



$$1.616255 \times 10^{-35} \text{ m}$$

Planck Scale



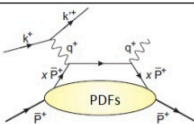
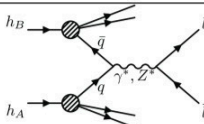
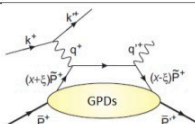
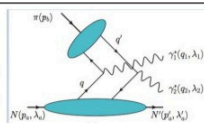
Hadrons are the bound state of quarks and gluons by strong interaction quantum chromodynamics (QCD).

- How actually quarks are distributed within hadrons or what is the internal structure of hadrons?
 - **Distribution functions**

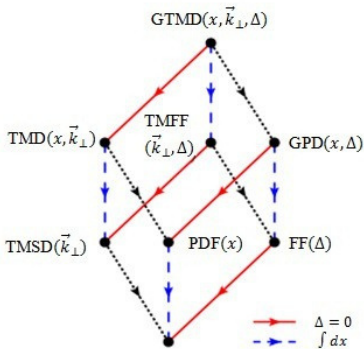
Distribution Functions (DFs)

- Describes the probability distribution of finding the constituents (quarks and gluons) within a hadron with physical observables.
- Information about longitudinal momentum, spatial location, momenta distributions, mechanical properties, structure of hadron etc.
- Used to study different decays of the the exclusive processes through some observables and compared with experimental data with evolutions.
- Some important DFs are generalized transverse momentum dependent distributions (GTMDs), transverse momentum dependent distribution functions (TMDs), generalized parton distributions (GPDs), parton distribution functions (PDFs) etc.

Distribution Functions

| PDFs | TMDs | GPDs | GTMDs |
|---|--|---|---|
| 1-D structure | 3-D structure | 3-D structure | 6-D structure |
| longitudinal distributions (x) | Both longitudinal (x) and transverse distribution (k_{\perp}) | longitudinal (x) and spatial distribution (ξ and Δ) | longitudinal (x), transverse (k_{\perp}), spatial distribution (ξ and Δ) with all DOF |
|  <p>DIS</p> |  <p>Drell-Yan process</p> |  <p>DVCS</p> |  <p>Double Drell - Yan</p> |

Distribution Functions



$$P = \left[P^+, \frac{4M^2 + \vec{\Delta}_T^2}{8(1 - \xi^2)P^+}, \vec{0}_T \right],$$

$$k = \left[xP^+, k^-, \vec{k}_T \right],$$

$$\Delta = \left[-2\xi P^+, \frac{4\xi M^2 + \xi \vec{\Delta}_T^2}{4(1 - \xi^2)P^+}, \vec{\Delta}_T \right],$$

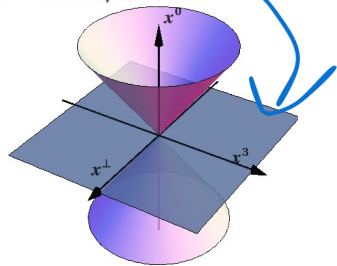
$$n = \left[0, \pm 1, \vec{0}_T \right].$$

- $x = \frac{k^+}{P^+}$ is the momentum fraction carried by the quark.
- k_\perp is the transverse momentum of quark.
- Δ is the momentum difference of the final and initial state of hadron.
- $\xi = -\frac{\Delta^+}{2P^+}$ is the skewness.

Light-front dynamics

Equal time quantization

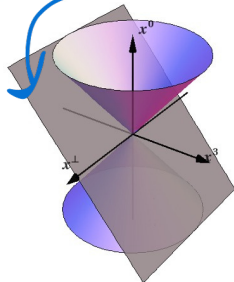
- time, $t = x^0$



- $x = (x^0, x^1, x^2, x^3)$ and $p = (p^0, p^1, p^2, p^3)$
- $i \frac{\partial |\psi(t)\rangle}{\partial t} = H |\psi(t)\rangle$
- Energy, $p^0 = \sqrt{m^2 + p^2}$

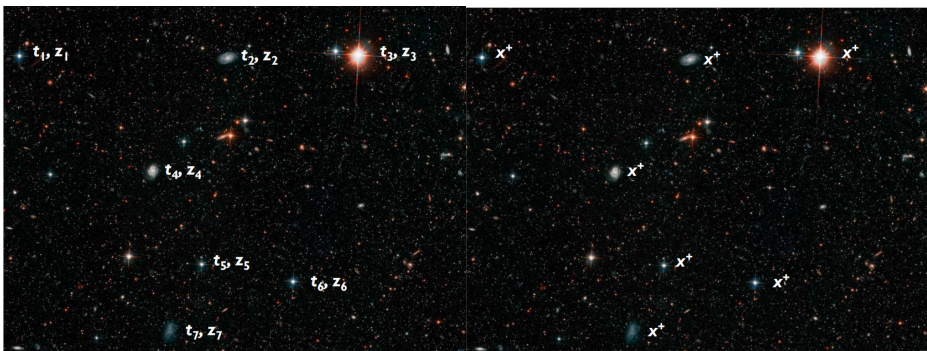
Light-front quantization

- time, $t = x^+ = x^0 + x^3$



- $x = (x^+, x^-, x^1, x^2)$ and $p = (p^+, p^-, p^1, p^2)$
- $i \frac{\partial |\psi(x^+)\rangle}{\partial x^+} = \frac{1}{2} p^- |\psi(x^+)\rangle$
- Energy, $p^- = \frac{m^2 + p_{\perp}^2}{p^+}$

Light-front dynamics



Instant Form

Front Form

Image from C. Lorce Talk

Why light-front ?

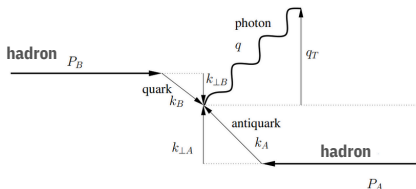
Ideal Framework to describe the hadronic structure. It can overcome many obstacles with many advantages.

- Simple vacume state
- Boost invariant frame
- Frame independent wave functions
- Hamiltonial formlism for relativistic bound state
- No square root in Hamiltonial p -
- Maximum number of kinematic variables



TMDs for Spin-0 Mesons

$$h_A(P_A) + h_B(P_B) \rightarrow \gamma^*(q) + X \rightarrow \ell^+(l) + \ell^-(l') + X$$



For spin-1 TMDs from DIS and SIDIS process. one can check Prof. A. Bachheta Papers
 Phys.Rev.D 62 (2000) 114004
 Phys.Lett.B 518 (2001) 85-93

Drell-Yan Process for hadrons

$$\begin{aligned} \frac{d\sigma^{DY}}{d|q_T|dydQ} &\simeq \frac{16\pi^2\alpha^2}{9Q^3} |q_T| F_{UU}^1(x_A, x_B, q_T, Q) \\ &= \frac{16\pi^2\alpha^2}{9Q^3} |q_T| \frac{x_A x_B}{2\pi} \mathcal{H}^{DY}(Q; \mu) \sum_a c_a(Q^2) \int d|b_T| |b_T| J_0(|q_T| |b_T|) \hat{f}_1^a(x_A, b_T^2; \mu, \zeta_A) \hat{f}_1^{\bar{a}}(x_B, b_T^2; \mu, \zeta_B), \end{aligned}$$

pseudorapidity

Hard factor

$$x_{A,B} = \frac{Q}{\sqrt{s}} e^{\pm y}$$

Structure Functions

Perturbative Evolutions

NP Quark TMDs

NP Anti-Quark TMDs

How to Access these TMDs ??

There are few methods to have an idea about pion TMDs

(1) Experiments

There is experimental data available for meson TMDs. However, COMPASS, EIC, May be upgrade 12 GeV JLab provide some data

(2) Lattice Simulations

Few lattice simulations study have been reported for the pion TMDs.
Arxiv: 2302.09961 (LPC), ArXiv:1506.07826

(3) Model Calculations

The non-perturbative constituent TMDs can be explored through low-energy models like LFM, BLFQ, NJL, DSE-BSE, and many more.

(4) Extractions & Fits

As there is no experimental data available. One can extract the TMDs from Drell-Yan cross section data (E615, E537 and NA70).

Arxiv: 2210.01733 (MAP Collaborations)

What we are doing ??

Model Calculations

We explore the spin-0 and spin-1 TMDs through NP models like LF models and NJL model (going On-)

We also evolve these TMDs to perturbative limits to predict for experiments through Collins-Soper-Sterman (CSS) evolutions.

Evacuate the PDFs from TMDs and their properties.

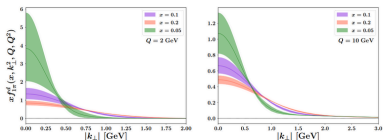
Explore the higher twist TMDs along with the higher Fock-state calculations (Going on-)

What about extractions ??

It is a challenging task to extract pion TMDs and PDFs from available experiments like E615, E537 and NA70 data.

Work going on.....

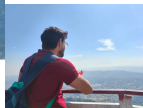
But Thanks God,
we have some extraordinary Computational Guys



Map Collaborations Pion Extractions



Mr. Hari (M.Sc Student)



Mr. Reetanshu (JRF)



Mr. Abhishek (M.Sc Student)

How to calculate ??

- In case of spin-0, pseudoscalar mesons, there are total 8 TMDs upto twist-4, which can be expressed in terms of quark-quark correlator as [S. Meissner, A. Metz, M. Schlegel and K. Goeke, JHEP 08, 038, (2008)]

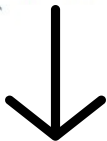
$$\Phi_q^{[\Gamma]}(x, \mathbf{k}_\perp) = \frac{1}{2} \int \frac{dz^- d^2 \vec{z}_\perp}{2(2\pi)^3} e^{i\mathbf{k}\cdot z} \langle \pi(K) | \bar{\psi}(0) \Gamma \mathcal{W}(0, z) \psi(z) | \pi(K) \rangle |_{z^+=0}.$$

Where $|\pi(K)\rangle$ is the LF bound state of pion/kaon with masses and momentum $M_{\pi(K)}$ and (P^+, P_\perp) respectively.

$\mathcal{W}(0, z)$ is the Wilson line which preserves the gauge invariance of the bilocal quark field operators in the correlation functions. For this work, we have taken it as unity.

Higher Twist TMDs

$$\frac{d\sigma}{d\Omega} \propto \left(1 + \lambda \cos^2 \theta + \mu \sin 2\theta \cos \phi + \frac{\nu}{2} \sin^2 \theta \cos 2\phi \right).$$



$$f_1(x, \vec{k}_T^2)$$

$$h_1^\perp(x, \vec{k}_T^2; \eta)$$

Twist-2



$$e(x, \vec{k}_T^2)$$

$$f^\perp(x, \vec{k}_T^2)$$

$$g^\perp(x, \vec{k}_T^2; \eta)$$

$$h(x, \vec{k}_T^2; \eta)$$

Twist-3



Unpolarized DY Cross Section

$$f_3(x, \vec{k}_T^2)$$

$$h_3^\perp(x, \vec{k}_T^2; \eta)$$

Twist-4

All TMDs for spin-0 mesons

Γ is the Dirac matrix which determines the Lorentz structure of the correlator $\Phi_q^{[\Gamma]}$. Depending upon the Γ , the TMDs are given as

| | T-even | T-odd |
|---------|--|--|
| Twist-2 | $\Phi[\gamma^+] = f_1^q(x, \mathbf{k}_\perp^2)$ | $\Phi[\sigma^{j+}\gamma_5] = \iota \frac{\epsilon^{ij} k_\perp^j}{M} h_1^\perp(x, \mathbf{k}_\perp^2)$ |
| Twist-3 | $\Phi[\gamma^1] = \frac{M}{P^+} e^q(x, \mathbf{k}_\perp^2)$ $\Phi[\gamma^j] = \frac{k_\perp^j}{P^+} f^\perp q(x, \mathbf{k}_\perp^2)$ | $\Phi[\gamma^j\gamma_5] = \iota \frac{\epsilon^{ij} k_\perp^i}{P^+} g^\perp(x, \mathbf{k}_\perp^2)$ $\Phi[\sigma^{ij}\gamma_5] = \iota \frac{M\epsilon^{ij}}{P^+} h(x, \mathbf{k}_\perp^2)$ |
| Twist-4 | $\Phi[\gamma^-] = \frac{M^2}{(P^+)^2} f_3^q(x, \mathbf{k}_\perp^2)$ | $\Phi[\sigma^{j-}\gamma_5] = \iota \frac{M\epsilon^{ijk_\perp^i}}{(P^+)^2} h_3^\perp(x, \mathbf{k}_\perp^2)$ |

- There are 4 T-even and 4 T-odd TMDs for spin-0 particles.
- All these T-even TMDs are unpolarized quark distributions.

S. Puhan, et.al, JHEP, 02, (2024).



Relations Among TMDs

- All the higher twist TMDs are related with leading twist TMD by

$$x e^q(x, \mathbf{k}_\perp^2) = x \tilde{e}^q(x, \mathbf{k}_\perp^2) + \frac{m_{q(\bar{q})}}{M} f_1^q(x, \mathbf{k}_\perp^2),$$

$$x f^{\perp q}(x, \mathbf{k}_\perp^2) = x \tilde{f}^{\perp q}(x, \mathbf{k}_\perp^2) + f_1^q(x, \mathbf{k}_\perp^2),$$

$$x^2 f_3^q(x, \mathbf{k}_\perp^2) = x^2 \tilde{f}_3^q(x, \mathbf{k}_\perp^2) + \frac{\mathbf{k}_\perp^2 + m_{q(\bar{q})}^2}{M^2} f_1^q(x, \mathbf{k}_\perp^2),$$

$$x g^\perp(x, \mathbf{k}_\perp^2) = x \tilde{g}^\perp(x, \mathbf{k}_\perp^2) + \frac{m_{q(\bar{q})}}{M} h_1^\perp(x, \mathbf{k}_\perp^2),$$

$$x h(x, \mathbf{k}_\perp^2) = x \tilde{h}(x, \mathbf{k}_\perp^2) + \frac{k_\perp^2}{M^2} h_1^\perp(x, \mathbf{k}_\perp^2),$$

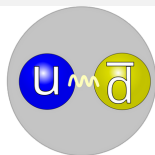
$$x^2 h_3^\perp(x, \mathbf{k}_\perp^2) = x^2 \tilde{h}_3^\perp(x, \mathbf{k}_\perp^2) + AF(\mathbf{k}_\perp^2) h_1^\perp(x, \mathbf{k}_\perp^2)$$

- In this work, we have adopted Wandzura-Wilczek approximation for valence quark calculations of T-even TMDs.

Light Mesons

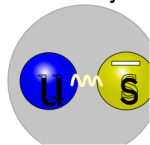
Pion

- Bound state of u- quark and d- antiquark.
- Having mass about 140 MeV. Exists only if mass is dynamically generated.



Kaon

- Bound state of u- quark and s- antiquark.
- Having mass about 490 MeV. Boundary between emergent and Higgs-mass mechanisms.

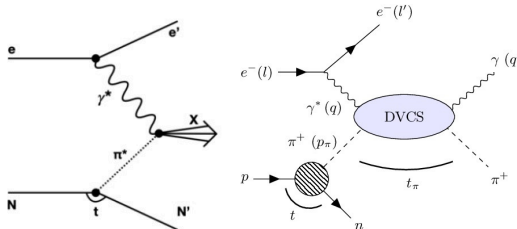


For the pion and the kaon the EIC will allow determination of the quark and gluon contributions to mass and internal structure through Sullivan Process.

[A.C. Aguilar et al., Pion and Kaon structure at the EIC, EPJA 55 (2019) 190.

J. Arrington et al., Revealing the structure of light pseudoscalar mesons at the EIC, J. Phys. G 48 (2021) 7 075106.]

Sullivan process



Sullivan

Hard scattering from virtual meson cloud of nucleon

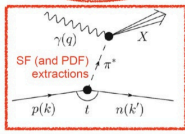
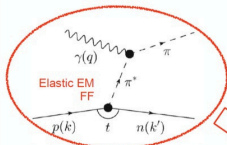
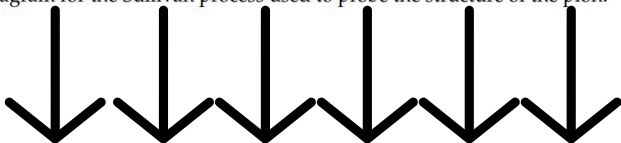


Diagram for the Sullivan process used to probe the structure of the pion.



➤ Accessing meson form factors through the Sullivan Process

- Extraction from data and validation of the technique
- F_{π^+} and F_{K^+} up to $Q^2 \sim 9$ and $\sim 6 \text{ GeV}^2$

Yellow EIC Report (2022)

Light cone quark model

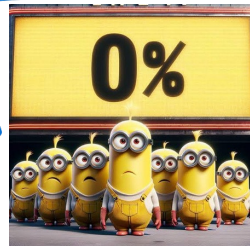
The Pion bound state wave function up to first principle

$$|\pi(P)\rangle = |\pi(P)\rangle_{q\bar{q}} + |\pi(P)\rangle_{q\bar{q}g} + |\pi(P)\rangle_{q\bar{q}gg} + \sum_{\{\bar{s}\bar{s}\}} |\pi(P)\rangle_{q\bar{q}\{\bar{s}\bar{s}\}},$$



Complicated! 😞

The unpolarized quark, gluon and sea quark PDF



$$f_1^v(x) = f_{1,q\bar{q}}^v(x) + f_{1,q\bar{q}g}^v(x) + f_{1,q\bar{q}gg}^v(x) + \sum_{\{\bar{s}\bar{s}\}} f_{1,q\bar{q}\{\bar{s}\bar{s}\}}^v(x),$$

$$f_1^g(x) = f_{1,q\bar{q}g}^g(x) + f_{1,q\bar{q}gg}^g(x),$$

$$f_1^S(x) = 2 \sum_{\{\bar{s}\bar{s}\}} f_{1,q\bar{q}\{\bar{s}\bar{s}\}}^S(x),$$

The Pion Form Factors

$$F_\pi(Q^2) = F_{\pi,q\bar{q}}(Q^2) + F_{\pi,q\bar{q}g}(Q^2) + F_{\pi,q\bar{q}gg}(Q^2) + \sum_{\{\bar{s}\bar{s}\}} F_{\pi,q\bar{q}\{\bar{s}\bar{s}\}}(Q^2),$$

Light cone quark model

The minimal Fock-state description of mesons in the form quark helicity λ for quark-antiquark is given by

$$|M(P, S_Z)\rangle = \sum_{\lambda_1, \lambda_2} \int \frac{dx d^2\mathbf{k}_\perp}{\sqrt{x(1-x)} 16\pi^3} \psi_{S_Z}(x, \mathbf{k}_\perp, \lambda_1, \lambda_2) |x, \mathbf{k}_\perp, \lambda_1, \lambda_2\rangle.$$

ψ_{S_Z} is the spin improved meson wave function written in the form

$$\psi_{S_Z}(x, \mathbf{k}_\perp, \lambda_1, \lambda_2) = \chi_{S_Z}(x, \mathbf{k}_\perp, \lambda_1, \lambda_2) \varphi(x, \mathbf{k}_\perp).$$

Momentum Space
Wave Functions
(BHL Prescriptions)

$$N_{\pi(K)} \left(1 + \frac{(x-1/2)^2 M_{\pi(K)}^2 + \mathbf{k}_\perp^2}{\beta_{\pi(K)}^2} \right)^{-s}.$$

Power-Law Wave functions

$$\varphi(x, \mathbf{k}_\perp) = A \exp \left[-\frac{\mathbf{k}_\perp^2 + m_q^2}{x} + \frac{\mathbf{k}_\perp^2 + m_{\bar{q}}^2}{1-x} - \frac{(m_q^2 - m_{\bar{q}}^2)^2}{8\beta^2 \left(\frac{\mathbf{k}_\perp^2 + m_q^2}{x} + \frac{\mathbf{k}_\perp^2 + m_{\bar{q}}^2}{1-x} \right)} + \frac{m_q^2 + m_{\bar{q}}^2}{4\beta^2} \right].$$

Light cone quark model

Melosh- Wigner Transformation
From
Instant-Form

$$\chi_{S_z}(x, \mathbf{k}_\perp, \downarrow, \uparrow) = -\frac{[(xM + m_q)((1-x)M + m_{\bar{q}}) - k_\perp^2]}{(\sqrt{2}\omega_1\omega_2)},$$

$$\chi_{S_z}(x, \mathbf{k}_\perp, \uparrow, \downarrow) = \frac{[(xM + m_q)((1-x)M + m_{\bar{q}}) - k_\perp^2]}{(\sqrt{2}\omega_1\omega_2)},$$

$$\chi_{S_z}(x, \mathbf{k}_\perp, \uparrow, \uparrow) = \frac{[(xM + m_q)q_2^L - ((1-x)M + m_{\bar{q}})q_1^L]}{(\sqrt{2}\omega_1\omega_2)},$$

$$\chi_{S_z}(x, \mathbf{k}_\perp, \downarrow, \downarrow) = \frac{[(xM + m_q)q_2^R - ((1-x)M + m_{\bar{q}})q_1^R]}{(\sqrt{2}\omega_1\omega_2)}.$$

Spin- Wave Functions

$$\omega_1 = [(xM + m_q)^2 + \mathbf{k}_\perp^2]^{\frac{1}{2}}, \omega_2 = [((1-x)M + m_{\bar{q}})^2 + \mathbf{k}_\perp^2]^{\frac{1}{2}}.$$

Light-Front Holographic Model

$$|M(P)\rangle = |M(P)\rangle_{L_z=0} + |M(P)\rangle_{|L_z|=1}. \quad \rightarrow \text{Mixing State Effect}$$

$$|M(P)\rangle_{L_z=0} = \int \frac{d^2\mathbf{k}_\perp}{16\pi^3} \frac{dx}{\sqrt{6x(1-x)}} \Psi^{(0)}(x, \mathbf{k}_\perp) \sum_{a=1}^3 \left[b_\uparrow^{\dagger a}(1) d_\downarrow^{\dagger a}(2) - b_\downarrow^{\dagger a}(1) d_\uparrow^{\dagger a}(2) \right] |0\rangle,$$

$$|M(P)\rangle_{|L_z|=1} = \int \frac{d^2\mathbf{k}_\perp}{16\pi^3} \frac{dx}{\sqrt{2x(1-x)}} \Psi^{(1)}(x, \mathbf{k}_\perp) \left(\frac{\mathbf{k}_\perp^+}{\sqrt{3}} \sum_{a=1}^3 b_\uparrow^{\dagger a}(1) d_\uparrow^{\dagger a}(2) |0\rangle + \frac{\mathbf{k}_\perp^-}{\sqrt{3}} \sum_{a=1}^3 b_\downarrow^{\dagger a}(1) d_\downarrow^{\dagger a}(2) |0\rangle \right).$$

Mixing State

Momentum Space Wave Functions

$$\Psi^{(0)}(x, \mathbf{k}_\perp) = -\frac{m_{q(\bar{q})} + Mx(1-x)}{\sqrt{2x(1-x)}} \psi(x, \mathbf{k}_\perp),$$


$$\Psi^{(1)}(x, \mathbf{k}_\perp) = -\frac{1}{\sqrt{2x(1-x)}} \psi(x, \mathbf{k}_\perp).$$

$$\psi(x, \mathbf{k}_\perp) = \frac{4\pi N}{\kappa\sqrt{x(1-x)}} \exp\left[-\frac{(\mathbf{k}_\perp^2 + (1-x)m_q^2 + xm_{\bar{q}}^2)}{2\kappa^2x(1-x)}\right].$$

The Leading Twist- TMD


Unpolarized Quark TMDs (T-even)

The leading twist f_1^q can be represent in the overlap form as

$$f_1^q(x, \mathbf{k}_\perp^2) = \frac{1}{16\pi^3} [|\psi_0(x, \mathbf{k}_\perp, \uparrow, \uparrow)|^2 + |\psi_0(x, \mathbf{k}_\perp, \downarrow, \downarrow)|^2 + |\psi_0(x, \mathbf{k}_\perp, \downarrow, \uparrow)|^2 + |\psi_0(x, \mathbf{k}_\perp, \uparrow, \downarrow)|^2].$$



LCQM

The overlap form of leading twist TMD is found to be

$$f_1^q(x, \mathbf{k}_\perp^2) = \frac{1}{(16\pi^3)} [|\Psi^{(0)}(x, \mathbf{k}_\perp)|^2 + |\Psi^{(1)}(x, \mathbf{k}_\perp)|^2].$$


LFHM

Boer-Mulders Quark TMD (T-odd)

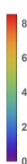
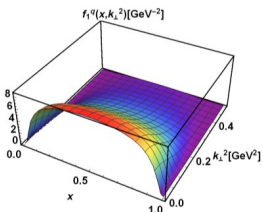
$$h_1^\perp(x, \mathbf{k}_\perp^2) = \frac{M_{\pi(K)}}{\mathbf{k}_\perp^2} \int \frac{d^2 \mathbf{k}'_\perp}{2(2\pi)^3} \text{Im}G(x, \mathbf{k}_\perp, \mathbf{k}'_\perp) \sum_{\lambda_1, \lambda_2} \left[(k_1 + ik_2) \left(\Psi_{\pi(K)}^*(x, \mathbf{k}'_\perp, \lambda_1, \downarrow) \Psi_{\pi(K)}(x, \mathbf{k}_\perp, \lambda_2, \uparrow) \right) - (k_1 - ik_2) \left(\Psi_{\pi(K)}^*(x, \mathbf{k}'_\perp, \lambda_1, \uparrow) \Psi_{\pi(K)}(x, \mathbf{k}_\perp, \lambda_2, \downarrow) \right) \right].$$


LCQM

$G(x, \mathbf{k}_\perp, \mathbf{k}'_\perp)$ is the initial state perturbative Abelian interaction operator for DY process and can be expressed as

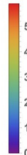
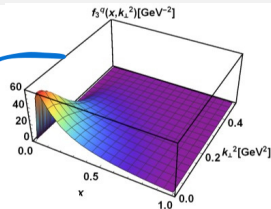
$$\text{Im}G(x, \mathbf{k}_\perp, \mathbf{k}'_\perp) = \frac{C_f \alpha_s}{2\pi} \frac{1}{(\mathbf{k}_\perp - \mathbf{k}'_\perp)^2}.$$

Our Findings for Pion u-quark

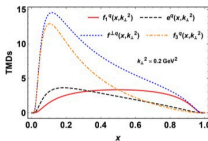
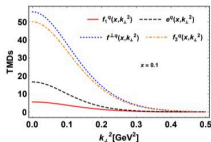


Twist-2 TMD

Twist-4 TMD

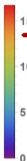
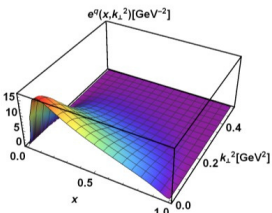


Due to
Factory of $1/x$

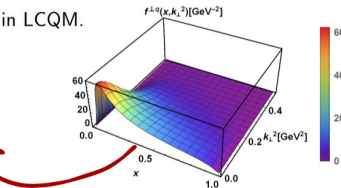


$$f_1^q(x, \mathbf{k}_\perp^2) \geq 0,$$

$$f_3^q(x, \mathbf{k}_\perp^2) \geq 0.$$



Twist-3 TMDs



Pion u-quark TMDs at a fixed x and in LCQM.

Our Findings for Pion

| pion | LCQM | | | LFHM | | | LFCM | | | BLFQ | |
|-----------|------------------------------------|--|-------|------------------------------------|--|-------|------------------------------------|--|-------|------------------------------------|--|
| | $\langle \mathbf{k}_\perp \rangle$ | $\langle \mathbf{k}_\perp^2 \rangle^{1/2}$ | R_G | $\langle \mathbf{k}_\perp \rangle$ | $\langle \mathbf{k}_\perp^2 \rangle^{1/2}$ | R_G | $\langle \mathbf{k}_\perp \rangle$ | $\langle \mathbf{k}_\perp^2 \rangle^{1/2}$ | R_G | $\langle \mathbf{k}_\perp \rangle$ | $\langle \mathbf{k}_\perp^2 \rangle^{1/2}$ |
| f_1 | 0.22 | 0.26 | 0.96 | 0.24 | 0.27 | 1.00 | 0.28 | 0.32 | 0.99 | 0.26 | 0.30 |
| e | 0.18 | 0.22 | 0.95 | 0.21 | 0.24 | 0.99 | 0.26 | 0.30 | 0.99 | 0.26 | 0.30 |
| f_\perp | 0.21 | 0.25 | 0.96 | 0.23 | 0.26 | 0.99 | 0.26 | 0.30 | 0.99 | 0.25 | 0.29 |
| f_s | 0.21 | 0.24 | 0.95 | 0.22 | 0.25 | 0.99 | 0.30 | 0.33 | 0.98 | - | - |



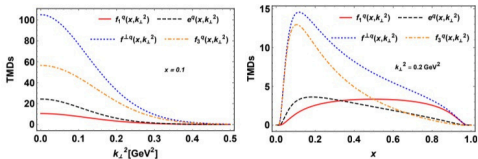
The Gaussian transverse dependence ratio of these TMDs to find the extent upto which the model supports Gaussian behavior as

$$R_G = \frac{2}{\sqrt{\pi}} \frac{\langle \mathbf{k}_\perp \rangle}{\langle \mathbf{k}_\perp^2 \rangle^{1/2}}$$

Our results almost similar to other model predictions.

We found that leading Twist TMD carry higher transverse Momenta which should be.

Our Findings for Kaon u-quark



Kaon u-quark TMDs at fixed values

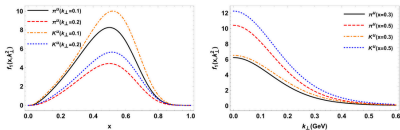
The transverse Gaussian Ratio found to deviate by 5 percentage from 1.

$$F^q(x, \mathbf{k}_\perp) = F^{\bar{q}}(1-x, -\mathbf{k}_\perp)$$

| u-quark | LCQM | | | LFHM | | |
|-----------|------------------------------------|--|-------|------------------------------------|--|-------|
| | $\langle \mathbf{k}_\perp \rangle$ | $\langle \mathbf{k}_\perp^2 \rangle^{\frac{1}{2}}$ | R_G | $\langle \mathbf{k}_\perp \rangle$ | $\langle \mathbf{k}_\perp^2 \rangle^{\frac{1}{2}}$ | R_G |
| f_1 | 0.26 | 0.30 | 0.98 | 0.24 | 0.27 | 1 |
| e | 0.21 | 0.25 | 0.96 | 0.21 | 0.24 | 0.99 |
| f^\perp | 0.23 | 0.27 | 0.96 | 0.22 | 0.25 | 0.99 |
| f_3 | 0.23 | 0.27 | 0.96 | 0.22 | 0.25 | 0.99 |
| s-quark | | | | | | |
| f_1 | 0.26 | 0.30 | 0.98 | 0.23 | 0.26 | 1 |
| e | 0.21 | 0.25 | 0.95 | 0.20 | 0.23 | 0.98 |
| f^\perp | 0.23 | 0.27 | 0.96 | 0.21 | 0.24 | 0.99 |
| f_3 | 0.18 | 0.21 | 0.97 | 0.19 | 0.22 | 0.97 |

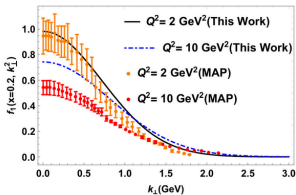
For Anti-Quark Distribution

Our Findings (Power-Law)

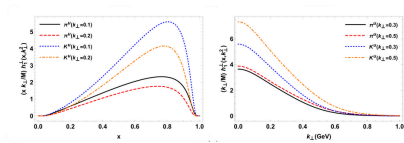


Unpolarized TMDs at Model Scale

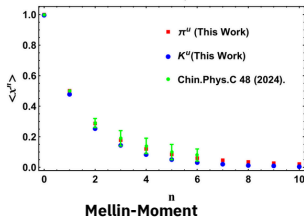
$$f_1(x, \mathbf{k}_\perp^2) - \frac{\mathbf{k}_\perp}{M_{\pi(K)}} h_\perp^1(x, \mathbf{k}_\perp^2) \geq 0$$



Unpolarized TMDs Evolutions using CSS
Compared with MAP Extraction Data



Boer-Mulders TMD at Model Scale



Different Wave compositions

For Spin-0 Mesons, the total wave function consists of S-wave and P-wave

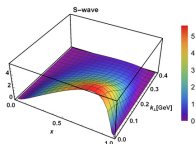
$$|M(P)\rangle = |M(P)\rangle_{L_z=0} + |M(P)\rangle_{|L_z|=1} \rightarrow \text{P-wave}$$

S-wave

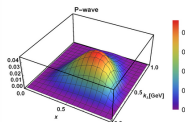
$$f_1(x, \mathbf{k}_\perp^2) = f_1^{(L_z=0)}(x, \mathbf{k}_\perp^2) + f_1^{(|L_z|=1)}(x, \mathbf{k}_\perp^2)$$

$$f_1^{(L_z=0)}(x, \mathbf{k}_\perp^2) = \frac{1}{6(2\pi)^3} |\psi_\pi(x, \mathbf{k}_\perp^2)|^2 (|\chi_\pi(x, \mathbf{k}_\perp^2, \uparrow, \downarrow)|^2 + |\chi_\pi(x, \mathbf{k}_\perp^2, \downarrow, \uparrow)|^2)$$

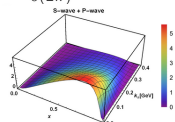
$$f_1^{(|L_z|=1)}(x, \mathbf{k}_\perp^2) = \frac{1}{6(2\pi)^3} |\psi_\pi(x, \mathbf{k}_\perp^2)|^2 (|\chi_\pi(x, \mathbf{k}_\perp^2, \uparrow, \uparrow)|^2 + |\chi_\pi(x, \mathbf{k}_\perp^2, \downarrow, \downarrow)|^2)$$



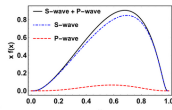
S-wave TMDs



P-wave TMDs



Total TMDs



PDFs

$$\langle \mathbf{k}_\perp^n \rangle = \int dx d^2 \mathbf{k}_\perp \mathbf{k}_\perp^n f_1(x, \mathbf{k}_\perp^2),$$

$$\langle x^n \rangle = \int dx d^2 \mathbf{k}_\perp x^n f_1(x, \mathbf{k}_\perp^2)$$

| | $\langle \mathbf{k}_\perp \rangle$ (GeV) | $\langle \mathbf{k}_\perp^2 \rangle$ (GeV ²) | $\langle x \rangle$ | $\langle x^2 \rangle$ | $\langle x^{-1} \rangle$ |
|-----------------|--|--|---------------------|-----------------------|--------------------------|
| S-wave | 0.21 | 0.06 | 0.47 | 0.28 | 2.63 |
| P-wave | 0.03 | 0.02 | 0.03 | 0.02 | 0.14 |
| S-wave + P-wave | 0.24 | 0.08 | 0.50 | 0.30 | 2.77 |

Our Findings for PDFs

$$f^{\perp q}(x) = \int d^2\mathbf{k}_{\perp} f^{\perp q}(x, \mathbf{k}_{\perp}^2)$$

$$f_1^q(x) = \int d^2\mathbf{k}_{\perp} f_1^q(x, \mathbf{k}_{\perp}^2),$$

$$e^q(x) = \int d^2\mathbf{k}_{\perp} e^q(x, \mathbf{k}_{\perp}^2),$$

$$f_3^q(x) = \int d^2\mathbf{k}_{\perp} f_3^q(x, \mathbf{k}_{\perp}^2).$$

PDFs upto
Twist-4

Obtained
Sum Rule

$$\int dx f_1^q(x) = N_q,$$

$$\sum_q \int dx x f_1^q(x) = 1,$$

$$\sum_q \int dx e^q(x) = \frac{\sigma_{\pi(K)}}{m_{q(\bar{q})}},$$

$$\int dx x e^q(x) = \frac{m_{q(\bar{q})}}{M_{\pi(K)}} N_q,$$

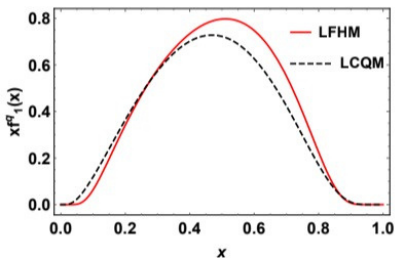
$$2 \int dx f_3^q(x) = N_q.$$

The above equation is called as
“quark-model Lorentz-invariance
relations (qLIRs)” for spin-0 PDFs.

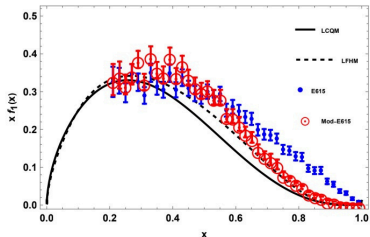
Eur.Phys.J.C 76 (2016) 7, 415

$$f_3^q(x) = \frac{f_1^q(x)}{2} + \frac{d}{dx} \int d^2\mathbf{k}_{\perp} \frac{\mathbf{k}_{\perp}^2}{2M_{\pi(K)}^2} f^{\perp q}(x, \mathbf{k}_{\perp}^2).$$

Our Findings for PDFs



**NLO DGLAP
Evolution**



0.205 GeV^2 \longrightarrow **16 GeV^2**

Ongoing

COMPASS++/

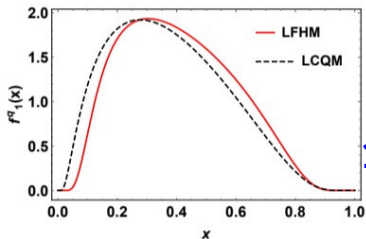
AMBER and

EIC.

**Pion u-Quark PDFs of both model
compared with experimental data**

E615 - J. S. Conway et al., Phys. Rev. D 39, 92 (1989). E615-Modified - M. Aicher et al., Phys. Rev. Lett. 105, 252003 (2010).

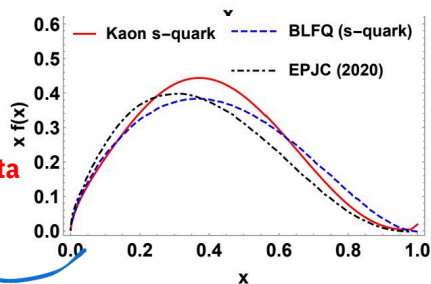
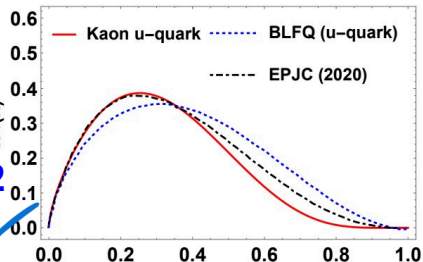
Our Findings for PDFs



**NLO DGLAP
Evolution
16 GeV²**

Kaon quark unpolarized PDFs evolved from 0.20 GeV² to 20 GeV² compared with [Phys.Rev.D 101 \(2020\)\[BLFQ\]](#) and [Eur. Phys. J. C 80, 1064 \(2020\)](#).

No experimental Data Available



Our Findings for PDFs

| | | |
|--------------------------|------|------|
| $\langle x^{-1} \rangle$ | LCQM | LFHM |
| $\pi^+(u\bar{d})$ | 2.79 | 2.62 |
| $K^+(u\bar{s})$ | 3.92 | 3.20 |

$$\langle x^{-1} \rangle_q = \int_0^1 dx \frac{f_1^{\pi(K)}(x)}{x}.$$

Inverse Momenta

**Average
Longitudinal
momentum
fraction
carried by
Quark**

| $\langle x \rangle$ | $f_1^q(x)$ | | $e^q(x)$ | | $f^{\perp}(x)$ | | $f_3^q(x)$ | |
|---------------------|------------|------|----------|------|----------------|------|------------|------|
| | LCQM | LFHM | LCQM | LFHM | LCQM | LFHM | LCQM | LFHM |
| $u(\pi^+)$ | 0.5 | 0.5 | 0.38 | 0.37 | 0.36 | 0.36 | 0.28 | 0.28 |
| $u(K^+)$ | 0.37 | 0.40 | 0.26 | 0.32 | 0.25 | 0.31 | 0.19 | 0.26 |

Table: Average longitudinal momentum fraction of pion and kaon
The leading twist PDFs carry higher longitudinal momentum fraction than higher twist PDFs.

In case of Kaon, the \bar{s} antiquark carry higher longitudinal momentum fraction than the u-quark.

At $Q^2 = 4 \text{ GeV}^2$, $\langle x \rangle$ is found to be 0.30 in LCQM which have very similar results with Lattice data and other models data.

TMDs for Spin-1 Particles

| Quark \ Hadron | U (γ^+) | | L ($\gamma^+\gamma_s$) | | T ($i\sigma^+\gamma_s / \sigma^+$) | |
|----------------|------------------|----------------|--------------------------|-------|--------------------------------------|------------------------------|
| | T-even | T-odd | T-even | T-odd | T-even | T-odd |
| U | f_1 | | | | | $[h_1^\perp]$ |
| L | | | g_{1L} | | | $[h_{1L}^\perp]$ |
| T | | f_{1T}^\perp | g_{1T} | | $[h_1], [h_{1T}^\perp]$ | |
| LL | f_{1LL} | | | | | $[h_{1LL}^\perp]$ |
| LT | f_{1LT} | | g_{1LT} | | | $[h_{1LT}], [h_{1LT}^\perp]$ |
| TT | f_{1TT} | | g_{1TT} | | | $[h_{1TT}], [h_{1TT}^\perp]$ |

Tensor TMDs

All Possible PDFs for Spin-1 Particles

| | $[\gamma^+]$ | | $[\gamma^+\gamma_s]$ | | $[i\sigma^+\gamma_s]$ | |
|----|--------------|--------|----------------------|--------|-----------------------|-------------|
| | TR-even | TR-odd | TR-even | TR-odd | TR-even | TR-odd |
| U | f_1 | | | | | |
| L | | | g_1 | | | |
| T | | | | | h_1 | |
| LL | f_{1LL} | | | | | |
| LT | | | | | | (h_{1LT}) |
| TT | | | | | | |

Extra For Spin-1 Particles Than Spin-1/2 Nucleons

Twist-2 TMD: $f_{1LL}, f_{1LT}, f_{1TT}, g_{1LT}, g_{1TT}, h_{1LL}^\perp, h_{1LT}^\perp, h_{1TT}^\perp, h_{1TT}, h_{1TT}^\perp,$

Twist-3 TMD: $f_{LL}^\perp, e_{LL}, f_{LT}^\perp, e_{LT}, e_{TT}^\perp, f_{TT}^\perp, e_{TT}, e_{TT}^\perp, g_{LL}^\perp, g_{LT}^\perp, g_{TT}^\perp, g_{TT}, g_{TT}^\perp, h_{1L}^\perp, h_{1LT}^\perp, h_{1TT}^\perp, h_{TT}, h_{TT}^\perp,$

Spin-1 leading twist TMDs

Source- S. Kumano and Q. T. Song, PLB 826 (2022)

Our Findings

$$e_{\Lambda(\mu)}^*(P)\langle\gamma^+\rangle_S^{\mu\nu}(x, \mathbf{k}_\perp^2)\epsilon_{\Lambda(\nu)}(P) = f_1(x, \vec{k}_\perp^2) + S_{LL}f_{1LL}(x, \vec{k}_\perp^2) + \frac{\vec{S}_{LT}\cdot\vec{k}_\perp}{M_\alpha}f_{1LT}(x, \vec{k}_\perp^2) + \frac{\vec{S}_{TT}\cdot\vec{k}_\perp}{M_\alpha^2}f_{1TT}(x, \vec{k}_\perp^2),$$

$$e_{\Lambda(\mu)}^*(P)\langle\gamma^+\gamma_5\rangle_S^{\mu\nu}(x, \mathbf{k}_\perp^2)\epsilon_{\Lambda(\nu)}(P) = S_L g_{1L}(x, \mathbf{k}_\perp^2) + \frac{\mathbf{k}_\perp\cdot\mathbf{S}_\perp}{M_\alpha}g_{1T}(x, \mathbf{k}_\perp^2),$$

TMDs Co-relator

$$e_{\Lambda(\mu)}^*(P)\langle\gamma^+\gamma^i\gamma_5\rangle_S^{\mu\nu}(x, \mathbf{k}_\perp^2)\epsilon_{\Lambda(\nu)}(P) = S^i h_\perp(x, \mathbf{k}_\perp^2) + S_\perp \frac{k_\perp^i}{2k_\perp^2} h_\perp^\perp(x, \mathbf{k}_\perp^2) + \frac{1}{2k_\perp^2} (2k_\perp^i \mathbf{k}_\perp\cdot\mathbf{S}_\perp - S^i \mathbf{k}_\perp^2) h_{1T}^\perp(x, \mathbf{k}_\perp^2),$$

$$A_{h_q^i \Lambda^i, h_q \Lambda}(x, \mathbf{k}_\perp^2) = \frac{1}{(2\pi)^3} \sum_{h_\bar{q}} \Psi_{h_q^i, h_q}^{(n)\Lambda^i*}(x, \mathbf{k}_\perp^2) \Psi_{h_q, h_q}^{(n)\Lambda}(x, \mathbf{k}_\perp^2).$$

Helicity
Amplitude

$$f_1(x, \mathbf{k}_\perp^2) = \frac{1}{6}(A_{+,+,0} + A_{-,-,0} + A_{+,+,+} + A_{-,-,-})$$

$$h_1(x, \mathbf{k}_\perp^2) = \frac{1}{4\sqrt{2}}(A_{+,-,0} + A_{-,-,+} + A_{+,-,-} + A_{-,-,0}),$$

$$g_{1L}(x, \mathbf{k}_\perp^2) = \frac{1}{4}(A_{+,+,+} - A_{-,-,+} - A_{+,-,+} + A_{-,-,-})$$

$$h_{1L}^\perp(x, \mathbf{k}_\perp^2) = \frac{M_\alpha}{4k_\perp^2}(k_R(A_{-,-,+} - A_{-,-,-}) + k_L(A_{+,-,+} - A_{+,-,-})),$$

$$g_{1T}(x, \mathbf{k}_\perp^2) = \frac{M_\alpha}{4\sqrt{2}k_\perp^2}(k_R(A_{+,+,0} - A_{-,-,0} + A_{+,-,+} - A_{-,-,-}) + k_L(A_{+,-,+} - A_{-,-,+} + A_{+,-,0} - A_{-,-,-}))$$

$$h_{1T}^\perp(x, \mathbf{k}_\perp^2) = \frac{M_\alpha^2}{2\sqrt{2}k_\perp^4}(k_R^2(A_{-,-,+} + A_{-,-,-}) + k_L^2(A_{+,-,+} + A_{+,-,-})),$$

$$f_{1LL}(x, \mathbf{k}_\perp^2) = \frac{1}{2}A_{+,+,0} + A_{-,-,0} - \frac{1}{4}(A_{+,+,+} + A_{-,-,+} + A_{+,-,+} + A_{-,-,-}),$$

$$f_{1LT}(x, \mathbf{k}_\perp^2) = \frac{M_\alpha}{4\sqrt{2}k_\perp^2}(k_R(A_{+,+,0} + A_{-,-,0} - A_{+,-,+} - A_{-,-,-}) + k_L(A_{+,-,+} + A_{-,-,+} - A_{+,-,0} - A_{-,-,0})),$$

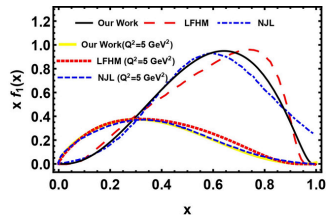
$$f_{1TT}(x, \mathbf{k}_\perp^2) = \frac{M_\alpha^2}{4\sqrt{2}k_\perp^4}(k_R^2(A_{+,-,+} + A_{-,-,-}) + k_L^2(A_{+,-,+} + A_{-,-,-})).$$

All Leading Twist

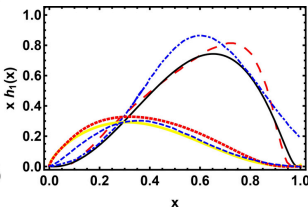
TMDs



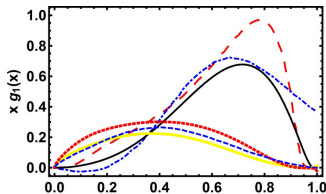
Rho meson PDFs



Unpolarized quark PDFs



transversity quark PDFs



helicity quark PDFs

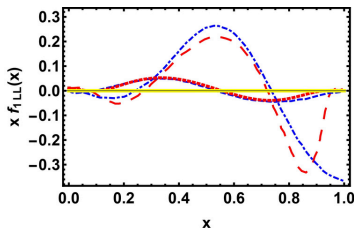
$$f_1(x) \geq 0$$

Positivity Constrains

$$\left(f_1(x) + \frac{2}{3}f_{1LL}(x)\right)\left(f_1(x) + g_1(x) - \frac{1}{3}f_{1LL}(x)\right) \geq 2|h_1(x)|^2$$

$$3f_1(x) \geq f_{1LL}(x) \geq -\frac{3}{2}f_1(x)$$

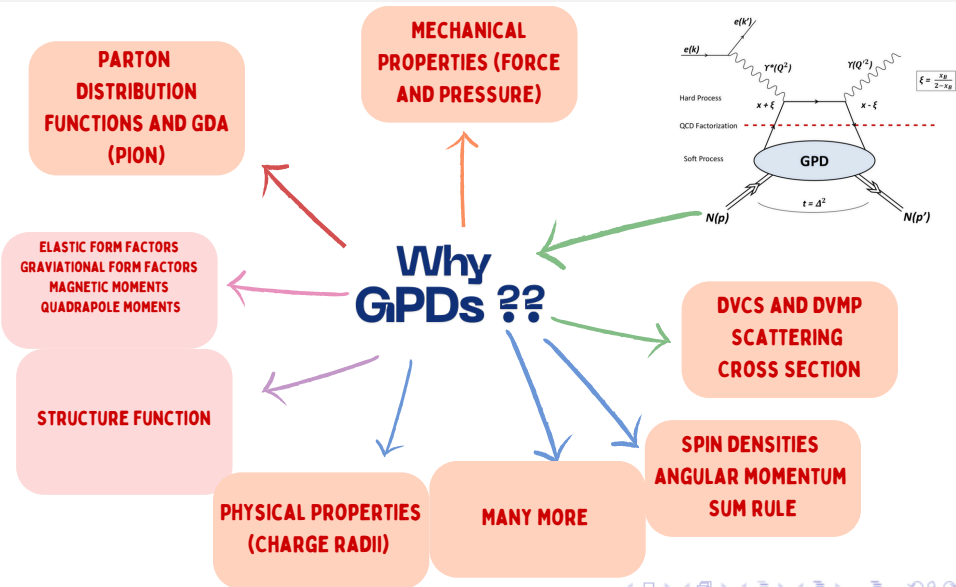
$$\frac{3}{2}f_1(x) \geq f_1(x) - \frac{1}{3}f_{1LL}(x) \geq |g_1(x)|$$



tensor quark PDFs

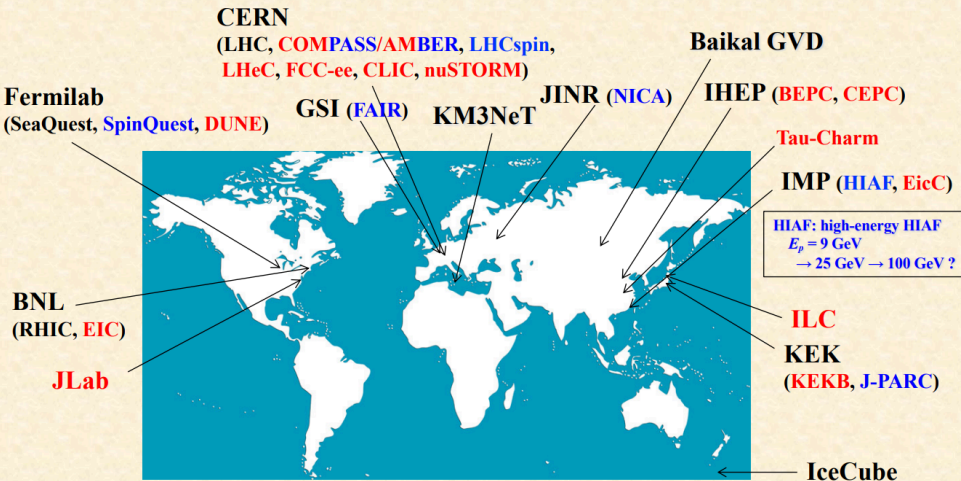
One can also Check out : Phys. Rev. C 96 (2017) 045206, Phys.Lett.B 851 (2024) 138563

Generalized Parton Distribution Function



Experimental Set up world wide

High-energy hadron physics experiments: hadron facilities



How Can we access them in Models ??

The quark-quark correlator for GPDs can be expressed as

$$F^{\Gamma}(x, \xi, t) = \int \frac{dz^-}{2\pi} e^{ik \cdot z} \left\langle p' \left| \bar{\psi} \left(-\frac{z}{2} \right) \Gamma \mathcal{W} \left(-\frac{z}{2}, \frac{z}{2} \right) \psi \left(\frac{z}{2} \right) \right| p \right\rangle_{z^+=0, z_T=0},$$

- P and P' are the initial and final hadron momenta.
- λ and λ' are the corresponding helicities.
- x is the average longitudinal momentum fraction of the parton.
- Γ represents the gamma matrix structure (e.g., γ^μ , $\gamma^\mu \gamma_5$, $\sigma^{\mu\nu}$) — this determines the type of GPD.

Variables

Momentum transfer: $\Delta = P' - P$, with $t = \Delta^2$.

Skewness: $\xi = \frac{P^+ - P'^+}{P^+ + P'^+}$, representing the difference in longitudinal momentum fractions.

Generalized Parton Distribution Function for Spin-0

Based on

Phys.Rev.D 111 (2025) 11, 114039 [S. Puhan & H. Dahiya]

Arxiv:2504.14982 [S. Puhan, S. Sharma,

N. Kumar & H. Dahiya]

There are total of 6 GPDs for the case of spin-0 mesons upto twist-4

$$\Phi_q^{[\Gamma]}(x, \xi, -\Delta_{\perp}^2) = \frac{1}{2} \int \frac{dz^-}{2\pi} e^{ik \cdot z} \langle \pi^+(K^+)(P^*, S_z = 0) | \bar{\psi}(-z/2) \Gamma W \psi(z/2) | \pi^+(K^+)(P, S_z = 0) \rangle |_{z^+ = z_{\perp} = 0},$$

$\Gamma = \{1, \gamma^j, \gamma^j \gamma^5, i\sigma^{ij} \gamma_5, \text{ or } \gamma^-, i\sigma^{j-} \gamma_5\}.$

Generalized Parton Distribution Function for Spin-0

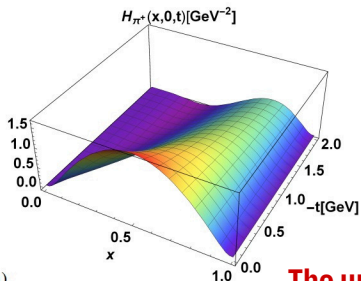
Vector GPD

$$\Phi_q^{[y^+]} = \frac{1}{2(2\pi)^3} \left[\Psi_\pi^*(x, \mathbf{k}'_\perp, \uparrow, \uparrow) \Psi_\pi(x, \mathbf{k}'_\perp, \uparrow, \uparrow) + \Psi_\pi^*(x, \mathbf{k}'_\perp, \downarrow, \uparrow) \Psi_\pi(x, \mathbf{k}'_\perp, \downarrow, \uparrow) \right. \\ \left. + \Psi_\pi^*(x, \mathbf{k}'_\perp, \uparrow, \downarrow) \Psi_\pi(x, \mathbf{k}'_\perp, \uparrow, \downarrow) + \Psi_\pi^*(x, \mathbf{k}'_\perp, \downarrow, \downarrow) \Psi_\pi(x, \mathbf{k}'_\perp, \downarrow, \downarrow) \right],$$

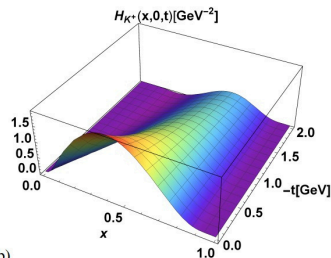
Transverse momenta

$$\mathbf{k}''_\perp = \mathbf{k}_\perp + (1-x) \frac{\Delta_\perp}{2}$$

$$\mathbf{k}'_\perp = \mathbf{k}_\perp - (1-x) \frac{\Delta_\perp}{2}$$



Information About D-term



The unpolarized GPDs at $\xi=0$

→ The longitudinal momentum fraction carried by the active quark decreases with increase in momentum transfer increase from initial hadron to final hadron.

Mechanical Property of Pion (D-term)

Why we need to Calculate ??

Highest pressure in nature 1 Pa (Pascal) = 1 N/m²



Earth atmosphere
10⁵ Pa = 1000 hPa



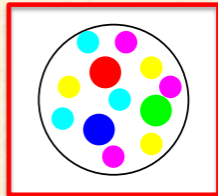
Center of earth
10¹¹ Pa = 100 GPa



Center of Sun
10¹⁶ Pa = 10 PPa



Neutron star
10³⁴ Pa



Hadron
10³⁵ Pa

How we can calculate ??

Energy-Momentum Tensor



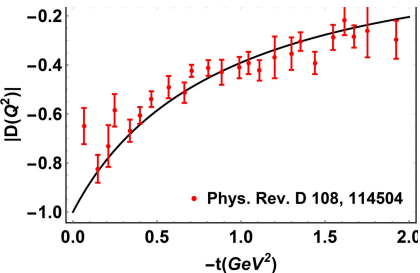
$$\langle p' | T^{\mu\nu} | p \rangle = \bar{u}(p') \left[A(Q^2) \gamma^{(\mu} P^{\nu)} + B(Q^2) \frac{i\sigma^{(\mu\alpha} \Delta_\alpha P^{\nu)}}{2M} + D(Q^2) \frac{\Delta^\mu \Delta^\nu - g^{\mu\nu} \Delta^2}{4M} \right] u(p)$$

$$\hat{T}_q^{\mu\nu}(x) = \frac{1}{4} \bar{\psi}_q(x) \left(i\gamma^\mu \overleftrightarrow{\partial}^\nu + i\gamma^\nu \overleftrightarrow{\partial}^\mu \right) \psi_q(x).$$

Mechanical property of pion

→ The pressure and shear distribution can be accessed from D-term of pion, which can also be calculated from GPDs.

$$\int_{-1}^1 dx x H(x, \xi, t) = A(t) + \xi^2 D(t)$$



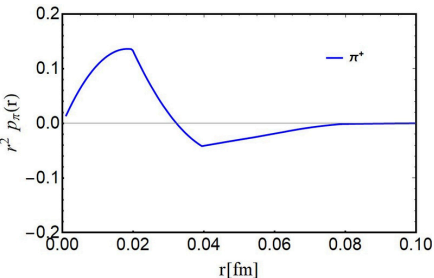
D-term of pion

**$|D(0)| = -1$ found to be in our case.
Recent Arxiv : [2504.14997](#), [2312.02543](#)
have obtained the same for pion.**

Mechanical property of pion

→ What about Pressure and Shear Distributions ??

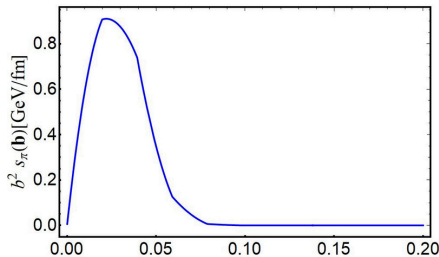
Pressure



$$p(r) = \frac{1}{6M} \frac{1}{r^2} \frac{d}{dr} \left(r^2 \frac{dD(r)}{dr} \right)$$

$$D(r) = \int \frac{d^3 \vec{q}}{(2\pi)^3} e^{i\vec{q}\cdot\vec{r}} D(Q^2) = \frac{1}{2\pi^2} \int_0^\infty dq q^2 \frac{\sin(qr)}{qr} D(Q^2)$$

Shear



$$s(r) = -\frac{1}{4M} \frac{1}{r} \frac{d}{dr} \left(\frac{1}{r} \frac{dD(r)}{dr} \right)$$

Mechanical property of pion

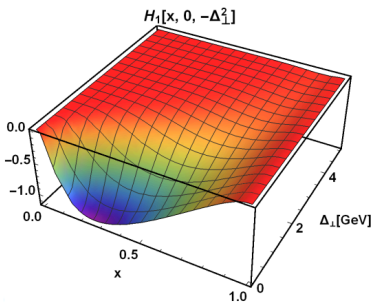
→ The pressure obey the stability condition

$$\int_0^{\infty} dr r^2 p(r) = 0$$

→ The maximum pressure inside the pion is found to be

$$1.0 \text{ GeV}/\text{fm}^3 = 1.602 \times 10^{35} \text{ Pa}$$

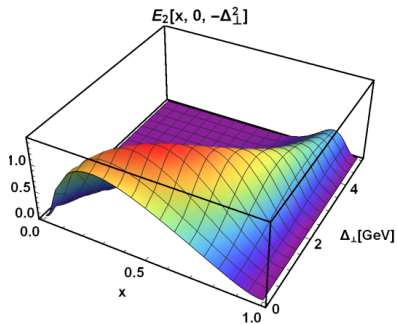
Other GPDs



Tensor GPD

Encodes helicity flip
processes

Spin-orbit Correlations



Scalar GPD

Contribute to Gravitational
Form Factors
dynamical chiral symmetry
breaking

Form Factors

$$\begin{aligned}
 F_v^q(Q^2) &= \int \frac{dx d^2\mathbf{k}_\perp}{16\pi^3} \left[\Psi_{\pi(K)}^*(x, \mathbf{k}'_\perp, \uparrow, \uparrow) \Psi_{\pi(K)}(x, \mathbf{k}'_\perp, \uparrow, \uparrow) + \Psi_{\pi(K)}^*(x, \mathbf{k}'_\perp, \uparrow, \downarrow) \Psi_{\pi(K)}(x, \mathbf{k}'_\perp, \uparrow, \downarrow) \right. \\
 &\quad \left. + \Psi_{\pi(K)}^*(x, \mathbf{k}'_\perp, \downarrow, \uparrow) \Psi_{\pi(K)}(x, \mathbf{k}'_\perp, \downarrow, \uparrow) + \Psi_{\pi(K)}^*(x, \mathbf{k}'_\perp, \downarrow, \downarrow) \Psi_{\pi(K)}(x, \mathbf{k}'_\perp, \downarrow, \downarrow) \right], \quad \mathbf{Vector} \\
 F_T^q(Q^2) &= \int \frac{dx d^2\mathbf{k}_\perp}{16\pi^3} \mathcal{M}_{\pi(K)} \left[i \left(\Psi_{\pi(K)}^*(x, \mathbf{k}'_\perp, \downarrow, \uparrow) \Psi_{\pi(K)}(x, \mathbf{k}'_\perp, \uparrow, \uparrow) + \Psi_{\pi(K)}^*(x, \mathbf{k}'_\perp, \downarrow, \downarrow) \Psi_{\pi(K)}(x, \mathbf{k}'_\perp, \uparrow, \downarrow) \right) \right. \\
 &\quad \left. - i \left(\Psi_{\pi(K)}^*(x, \mathbf{k}'_\perp, \uparrow, \uparrow) \Psi_{\pi(K)}(x, \mathbf{k}'_\perp, \downarrow, \uparrow) + \Psi_{\pi(K)}^*(x, \mathbf{k}'_\perp, \uparrow, \downarrow) \Psi_{\pi(K)}(x, \mathbf{k}'_\perp, \downarrow, \downarrow) \right) \right], \quad \mathbf{Tensor} \\
 F_S^q(Q^2) &= \int \frac{dx d^2\mathbf{k}_\perp}{\mathcal{M}_{\pi(K)} 16\pi^3} \left[\frac{m_q}{x} \left(\Psi_{\pi(K)}^*(x, \mathbf{k}'_\perp, \uparrow, \uparrow) \Psi_{\pi(K)}(x, \mathbf{k}'_\perp, \uparrow, \uparrow) + \Psi_{\pi(K)}^*(x, \mathbf{k}'_\perp, \uparrow, \downarrow) \Psi_{\pi(K)}(x, \mathbf{k}'_\perp, \uparrow, \downarrow) \right) \right. \\
 &\quad \left. + \Psi_{\pi(K)}^*(x, \mathbf{k}'_\perp, \downarrow, \uparrow) \Psi_{\pi(K)}(x, \mathbf{k}'_\perp, \downarrow, \uparrow) + \Psi_{\pi(K)}^*(x, \mathbf{k}'_\perp, \downarrow, \downarrow) \Psi_{\pi(K)}(x, \mathbf{k}'_\perp, \downarrow, \downarrow) \right) \quad \mathbf{Scalar} \\
 &\quad + \frac{(\Delta_1 + i\Delta_2)}{2x} \left(\Psi_{\pi(K)}^*(x, \mathbf{k}'_\perp, \downarrow, \uparrow) \Psi_{\pi(K)}(x, \mathbf{k}'_\perp, \uparrow, \uparrow) + \Psi_{\pi(K)}^*(x, \mathbf{k}'_\perp, \downarrow, \downarrow) \Psi_{\pi(K)}(x, \mathbf{k}'_\perp, \uparrow, \downarrow) \right) \\
 &\quad \left. - \frac{(\Delta_1 - i\Delta_2)}{2x} \left(\Psi_{\pi(K)}^*(x, \mathbf{k}'_\perp, \uparrow, \uparrow) \Psi_{\pi(K)}(x, \mathbf{k}'_\perp, \downarrow, \uparrow) + \Psi_{\pi(K)}^*(x, \mathbf{k}'_\perp, \uparrow, \downarrow) \Psi_{\pi(K)}(x, \mathbf{k}'_\perp, \downarrow, \downarrow) \right) \right].
 \end{aligned}$$

Quark Form Factors

Total Form Factors

$$F_M(-t) = e_q F_{M_q}(-t) + e_{\bar{q}} F_{M_{\bar{q}}}(-t).$$


Form Factors

Explicit form Found to be

$$F_V^{q(\pi)}(Q^2) = \int \frac{dx d^2\mathbf{k}_\perp}{16\pi^3} \left[\mathbf{k}_\perp^2 - (1-x)^2 \frac{\Delta_\perp^2}{4} + (m_u(1-x) + xm_{\bar{d}})^2 \right] \frac{\psi_\pi^*(x, \mathbf{k}'_\perp) \psi_\pi(x, \mathbf{k}_\perp)}{\omega''_\pi \omega'_\pi},$$

$$F_T^{q(\pi)}(Q^2) = \int \frac{dx d^2\mathbf{k}_\perp}{16\pi^3} \left[\mathcal{M}_\pi(1-x)(m_u(1-x) + m_{\bar{d}}x) \right] \frac{\psi_\pi^*(x, \mathbf{k}'_\perp) \psi_\pi(x, \mathbf{k}_\perp)}{\omega''_\pi \omega'_\pi},$$

$$F_S^{q(\pi)}(Q^2) = \int \frac{dx d^2\mathbf{k}_\perp}{16\pi^3} \frac{2m_u}{x\mathcal{M}_\pi} \left[\mathbf{k}_\perp^2 - (1-x)^2 \frac{\Delta_\perp^2}{4} + (m_u(1-x) + xm_{\bar{d}})^2 + m_u(1-x)\Delta_\perp^2 \right] \frac{\psi_\pi^*(x, \mathbf{k}'_\perp) \psi_\pi(x, \mathbf{k}_\perp)}{\omega''_\pi \omega'_\pi},$$



$$\omega''_\pi = (\mathcal{M}''_\pi + m_u + m_{\bar{d}}) \sqrt{x(1-x)[\mathcal{M}''_\pi{}^2 - (m_u - m_{\bar{d}})^2]},$$

$$\omega'_\pi = (\mathcal{M}'_\pi + m_u + m_{\bar{d}}) \sqrt{x(1-x)[\mathcal{M}'_\pi{}^2 - (m_u - m_{\bar{d}})^2]}.$$

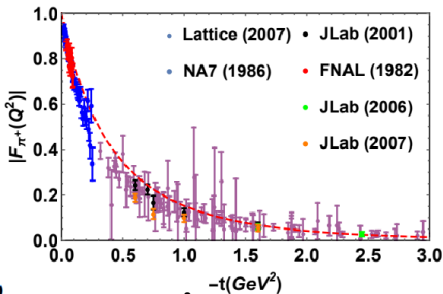
$$\mathcal{M}''_\pi = \sqrt{\frac{(\mathbf{k}_\perp - \frac{\Delta_\perp}{2})^2 + m_u^2}{x} + \frac{(\mathbf{k}_\perp - \frac{\Delta_\perp}{2})^2 + m_{\bar{d}}^2}{1-x}},$$

$$\mathcal{M}'_\pi = \sqrt{\frac{(\mathbf{k}_\perp + \frac{\Delta_\perp}{2})^2 + m_u^2}{x} + \frac{(\mathbf{k}_\perp + \frac{\Delta_\perp}{2})^2 + m_{\bar{d}}^2}{1-x}}.$$



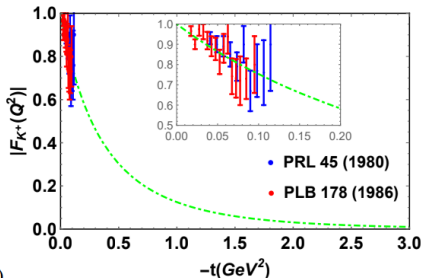
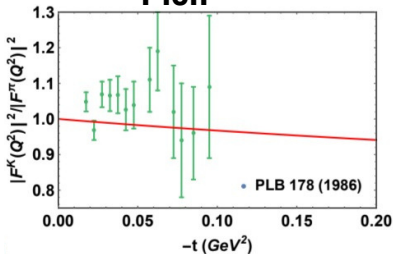
**Final and
Initial
bound state mass**

Vector FFs



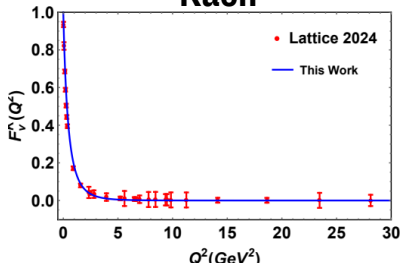
(a)

Pion



(b)

Kaon

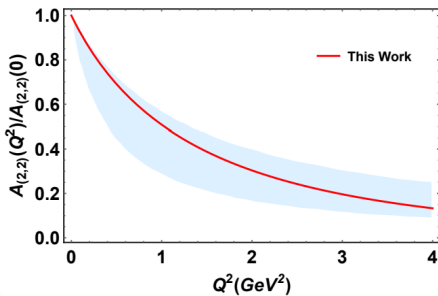
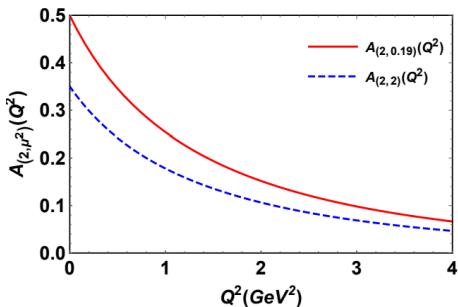


Vector Form Factors of Pion

Second Moment of Vector FFs

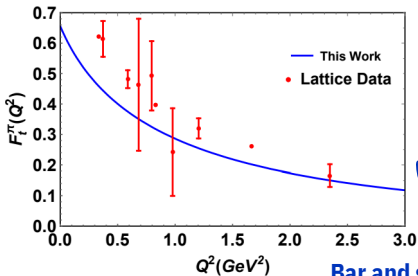
(Phys.Lett.B 747 (2015) 460-467)

$$A_2(Q^2) = \int dx x F_1(x, 0, -\Delta_\perp^2),$$

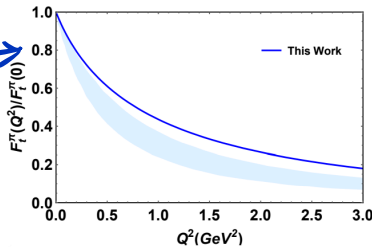


Shaded region- Lattice 2007

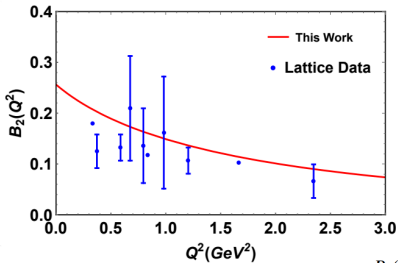
Tensor Form Factors of Pion



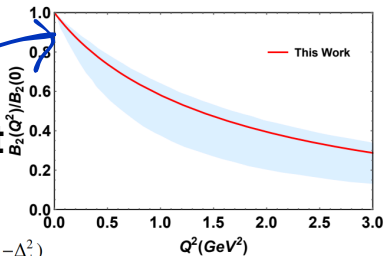
**First
Moment**



Bar and shaded regions are from Lattice 2007

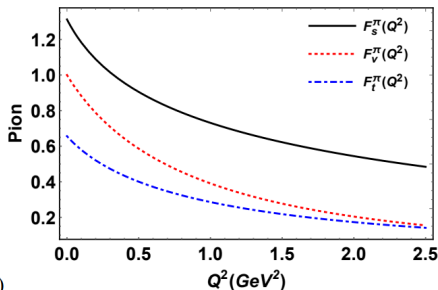


**Second
Moment**



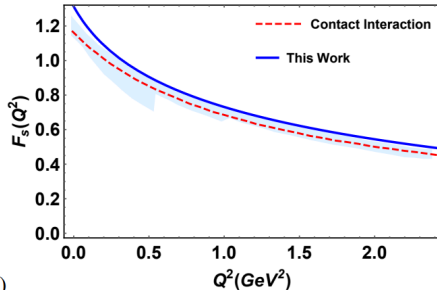
$$B_2(Q^2) = \int dx x H_1(x, 0, -\Delta_\perp^2)$$

Scalar Form Factors



(a)

Scalar, Vector and
Tensor FFs of pion



(b)

Scalar FF have been compared with Phys.
Rev. D 106, 054016 (CI) and
PhysRevD.105.054502 (Shaded Region)

$$\rightarrow F_S^{\pi(K)}(Q^2) \geq F_V^{\pi(K)}(Q^2) \geq F_T^{\pi(K)}(Q^2)$$

Scalar FF has higher distributions compared to other FFs

Charge radii

Charge radii corresponds to different FFs can be calculated as

$$\langle r_S^2 \rangle = \frac{-6}{F_S(0)} \frac{\partial F_S(Q^2)}{\partial Q^2} \Big|_{Q^2 \rightarrow 0} \quad \text{—————} \quad \text{Scalar Radii}$$


$$\langle r_V^2 \rangle = \frac{-6}{F_V(0)} \frac{\partial F_V(Q^2)}{\partial Q^2} \Big|_{Q^2 \rightarrow 0} \quad \text{—————} \quad \text{Vector Radii}$$

$$\langle r_T^2 \rangle = \frac{-6}{F_T(0)} \frac{\partial F_T(Q^2)}{\partial Q^2} \Big|_{Q^2 \rightarrow 0} \quad \text{—————} \quad \text{Tensor Radii}$$

All are in units of fermi meter

Charge radii Compared with available predictions

| | Pion | | | u-quark (Kaon) | | | s-antiquark (K) | | | Kaon | | |
|-----------------|--------------------------------|--------------------------------|--------------------------------|--------------------------------|--------------------------------|--------------------------------|--------------------------------|--------------------------------|--------------------------------|--------------------------------|--------------------------------|--------------------------------|
| | $\sqrt{\langle r_S^2 \rangle}$ | $\sqrt{\langle r_V^2 \rangle}$ | $\sqrt{\langle r_T^2 \rangle}$ | $\sqrt{\langle r_S^2 \rangle}$ | $\sqrt{\langle r_V^2 \rangle}$ | $\sqrt{\langle r_T^2 \rangle}$ | $\sqrt{\langle r_S^2 \rangle}$ | $\sqrt{\langle r_V^2 \rangle}$ | $\sqrt{\langle r_T^2 \rangle}$ | $\sqrt{\langle r_S^2 \rangle}$ | $\sqrt{\langle r_V^2 \rangle}$ | $\sqrt{\langle r_T^2 \rangle}$ |
| This Work | 0.528 | 0.558 | 0.567 | 0.440 | 0.663 | 0.605 | 0.338 | 0.406 | 0.326 | 0.409 | 0.568 | 0.529 |
| LQCD [50] | 0.482 | 0.539 | 0.679 | 0.386 | - | 0.618 | 0.321 | - | 0.5 | - | 0.538 | - |
| CI-MRL [56] | 0.434 | 0.558 | 0.583 | - | - | - | - | - | - | - | - | - |
| Ref. [80] | - | 0.640 | - | - | - | - | - | - | - | - | 0.530 | - |
| NA7 [29, 81] | - | 0.657, 0.662 | - | - | - | - | - | - | - | - | - | - |
| JLQCD [82] | - | 0.677 | - | - | - | - | - | - | - | - | 0.616 | - |
| CERN-NA007 [40] | - | - | - | - | - | - | - | - | - | - | 0.583 | - |
| PDG [83] | - | 0.659 | - | - | - | - | - | - | - | - | 0.560 | - |
| LQCD [84] | 0.635 | - | - | - | - | - | - | - | - | - | - | - |
| Ref. [79] | - | 0.65 | - | - | 0.62 | - | - | 0.43 | - | - | - | - |


 $\sqrt{\langle r_T^2 \rangle}(fm) \geq \sqrt{\langle r_V^2 \rangle}(fm) \geq \sqrt{\langle r_S^2 \rangle}(fm).$

For Pion

Same as CI-MRL, PhysRevD.106.054016

Spin-1 GPDs

Why necessary ??

Based on Arxiv:2505.09213

Very Less Theoretical Study available

Spin polarizations make more interesting

Only one HERMES data available for Structure functions

Tensor Structure (Absent for nucleons and spin-0 mesons)

Eur. Phys. J. A 19, 023–028 (2004)
DOI 10.1140/epj/A/2003/0023-aTHE EUROPEAN
PHYSICAL JOURNAL A

VOLUME 37, NUMBER 14

PHYSICAL REVIEW LETTERS

1 OCTOBER 2001

Deep electroproduction of photons and mesons on the deuteron

F. Cizef and B. Pire^{1,2*}¹ ILLUMINUS/SPIN, CEA-Saclay, F-91191 Gif-sur-Yvette Cedex, France² CPAT, Ecole Polytechnique, CNRS (UMI 6585), F-91128 Palaiseau Cedex, FranceReceived: 22 July 2003 / Revised version: 9 September 2003 /
Published online: 5 February 2004 – © Società Italiana di Fisica / Springer-Verlag 2004
Communicated by V. Vento

Generalized Parton Distributions in the Deuteron

E. R. Berger¹, F. Cizef¹, M. Diehl^{1,2} and B. Pire¹

CPAT, Ecole Polytechnique, F-91128 Palaiseau, France

ILLUMINUS/SPIN, CEA-Saclay, F-91191 Gif-sur-Yvette Cedex, France

¹Observatoire Hadronique-Structure DESY, D-22607 Hamburg, Germany

(Received 30 June 2001; published 17 September 2001)

We introduce generalized spin and gluon distributions in the deuteron, which can be measured in exclusive processes. We discuss virtual Compton scattering and meson electroproduction. We discuss the basic properties of these distributions and point out how they probe the interplay of nucleon and parton degrees of freedom in the deuteron wave function.

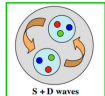
DOI: 10.1103/PhysRevLett.87.142002

PACS numbers: 24.85.+g, 12.38.Bx, 13.80.Fv

Deuteron spin structure functions at small Bjorken x J. Eidebrann, G. Piller, and W. Weise
Physik Department, Technische Universität München, D-85747 Garching, Germany
(Received 25 September 1997)We investigate related deuteron structure functions at small values of the Bjorken variable, $x < 0.1$. In this region contributions from the coherent interaction of diffractively excited hadronic states with both nucleons become important. A proper treatment of this process requires an extension of the Glauber-Gribov multiplescattering theory to include spin degrees of freedom. In the kinematic domain of current fixed target experiments we observe that shadowing effects in g_1^d are approximately twice as large as for the unpolarized structure function F_2^d . Furthermore at $x < 0.1$ the tensor structure function b_1 is found to receive significant contributions from coherent double scattering. [S0556-2813(1998)02596-4]

PACS number(s): 13.60.Bb, 24.70.+g, 25.10.+g

Spin-1 deuteron

only S wave
 $b_1=0$ standard model $b_1 \neq 0$

New hadronic mechanism?!

 b_1 experiment
 $\neq b_1$ "standard model"

Source: S. Kumano slides

Spin-1 GPDs

There are total 9 GPDs for the case of spin-1 vector mesons, out of which 5 are unpolarized GPDs

Unpolarized GPDs

$$\begin{aligned}
 V_{\lambda'\lambda} &= \int \frac{d\kappa}{2\pi} e^{ix\kappa 2\bar{P}\cdot n} \langle P', \lambda' | \bar{\psi}(-\kappa n) \gamma \cdot n \psi(\kappa n) | P, \lambda \rangle \\
 &= \sum_{i=1,5} \epsilon'^{* \beta} V_{\beta\alpha}^{(i)} \epsilon^\alpha H_i(x, \xi, t),
 \end{aligned}$$

Polarized GPDs

$$\begin{aligned}
 A_{\lambda'\lambda} &= \int \frac{d\kappa}{2\pi} e^{ix\kappa 2\bar{P}\cdot n} \langle P', \lambda' | \bar{\psi}(-\kappa n) \gamma \cdot n \gamma_5 \psi(\kappa n) | P, \lambda \rangle \\
 &= \sum_{i=1,4} \epsilon'^{* \beta} A_{\beta\alpha}^{(i)} \epsilon^\alpha \tilde{H}_i(x, \xi, t),
 \end{aligned}$$

Spin-1 Unpolarized GPDs

The LF overlap correlation function

$$\begin{aligned}
 V_{S'_z, S_z}(x, 0, -\Delta_\perp^2) = & -(\epsilon'^* \cdot \epsilon)H_1(x, 0, -\Delta_\perp^2) + \frac{(\epsilon \cdot n)(\epsilon' \cdot P) + (\epsilon' \cdot n)(\epsilon \cdot P)}{P \cdot n}H_2(x, 0, -\Delta_\perp^2) \\
 & -2\frac{(\epsilon \cdot P)(\epsilon'^* \cdot P)}{M_{q\bar{q}}^2}H_3(x, 0, -\Delta_\perp^2) + \frac{(\epsilon \cdot n)(\epsilon' \cdot P) - (\epsilon'^* \cdot n)(\epsilon \cdot P)}{P \cdot n}H_4(x, 0, -\Delta_\perp^2) \\
 & + \left\{ M_{q\bar{q}}^2 \frac{(\epsilon \cdot n)(\epsilon' \cdot n)}{(P \cdot n)^2} + \frac{1}{3}(\epsilon'^* \cdot \epsilon) \right\} H_5(x, 0, -\Delta_\perp^2),
 \end{aligned}$$

All the GPDs is found to be

$$\begin{aligned}
 H_1(x, 0, -\Delta_\perp^2) = & \frac{1}{3}[V_{0,0}(x, 0, -\Delta_\perp^2) - 2(\eta - 1)V_{1,1}(x, 0, -\Delta_\perp^2) \\
 & + 2\sqrt{2\eta}V_{1,0}(x, 0, -\Delta_\perp^2) + 2V_{1,-1}(x, 0, -\Delta_\perp^2)],
 \end{aligned}$$

$$H_2(x, 0, -\Delta_\perp^2) = 2V_{1,1}(x, 0, -\Delta_\perp^2) - \frac{2}{\sqrt{2\eta}}V_{1,0}(x, 0, -\Delta_\perp^2),$$

$$H_3(x, 0, -\Delta_\perp^2) = -\frac{V_{1,-1}(x, 0, -\Delta_\perp^2)}{\eta}, \quad V_{S'_z, S_z}(x, 0, -\Delta_\perp^2) = \sum_{\lambda_1, \lambda_2} \int \frac{d^2\mathbf{k}_\perp}{2(2\pi)^3} \Psi_{S'_z}^*(x, \mathbf{k}'_\perp, \lambda_1, \lambda_2) \Psi_{S_z}(x, \mathbf{k}_\perp, \lambda_1, \lambda_2).$$

$$H_4(x, 0, -\Delta_\perp^2) = 0,$$

$$H_5(x, 0, -\Delta_\perp^2) = V_{0,0}(x, 0, -\Delta_\perp^2) - (1 + 2\eta)V_{1,1} + 2\sqrt{2\tau}V_{1,0}(x, 0, -\Delta_\perp^2) - V_{1,-1}(x, 0, -\Delta_\perp^2).$$

With

Spin-1 Unpolarized GPDs

Here, $\eta = \frac{\Delta_\perp^2}{4M_{q\bar{q}}^2}$. Consequently, the LF overlap correlation function $V_{S'_z, S_z}(x, \xi, -\Delta_\perp^2)$ obey the parity and time reversal invariance as

$$V_{S'_z, S_z}(x, 0, -\Delta_\perp^2) = (-1)^{S'_z - S_z} V_{-S'_z, -S_z}(x, 0, -\Delta_\perp^2),$$

$$V_{S'_z, S_z}(x, \xi, -\Delta_\perp^2) = (-1)^{S'_z - S_z} V_{S'_z, S_z}(x, -\xi, -\Delta_\perp^2).$$

$$n = (0, \sqrt{2}, 0, 0),$$

$$\Delta = (0, 0, \Delta_\perp, 0),$$

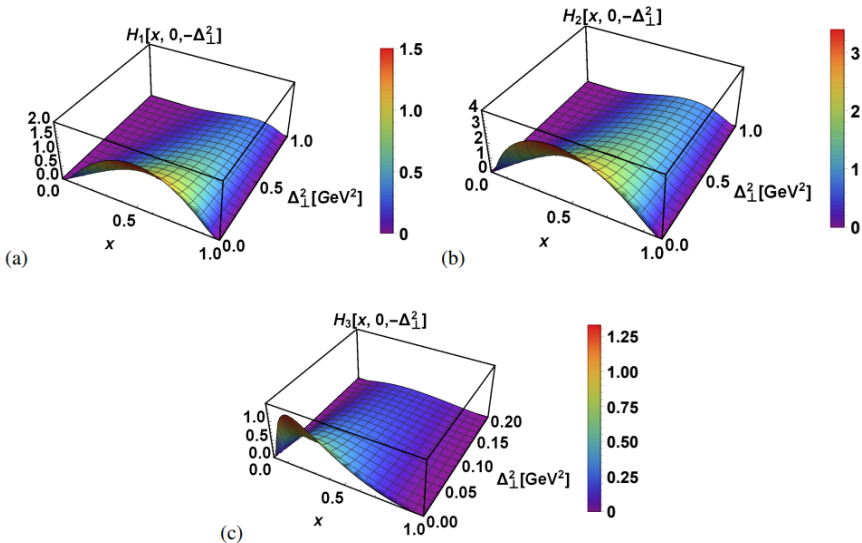
$$P = \frac{M_{q\bar{q}}}{\sqrt{2}} \left(\sqrt{1+\eta}, \sqrt{1+\eta}, -\frac{\Delta_\perp}{M_{q\bar{q}} \sqrt{2}}, 0 \right)$$

$$P' = \frac{M_{q\bar{q}}}{\sqrt{2}} \left(\sqrt{1+\eta}, \sqrt{1+\eta}, \frac{\Delta_\perp}{M_{q\bar{q}} \sqrt{2}}, 0 \right).$$



Taken Four-vector notations

Spin-1 Unpolarized GPDs



Spin-1 Form Factors

There are total 3 FFs present for the spin-1 unpolarized case, which can be solved through

$$\langle M(P^{+'}, S_z' | J^\mu | M(P^+, \mathbf{P}_\perp, S_z) \rangle = -\epsilon' \cdot \epsilon (P + P')^\mu F_1(Q^2) + (\epsilon' n \cdot \epsilon' - \epsilon' n \cdot \epsilon) F_2(Q^2) + \frac{(\epsilon' \cdot n)(\epsilon \cdot n)}{2M_v^2} (P + P')^\mu F_3(Q^2),$$

Through Spin-1 GPDs as

$$\int_{-1}^1 dx H_i(x, 0, -\Delta_\perp^2) = F_i(Q^2), \quad (i = 1, 2, 3)$$

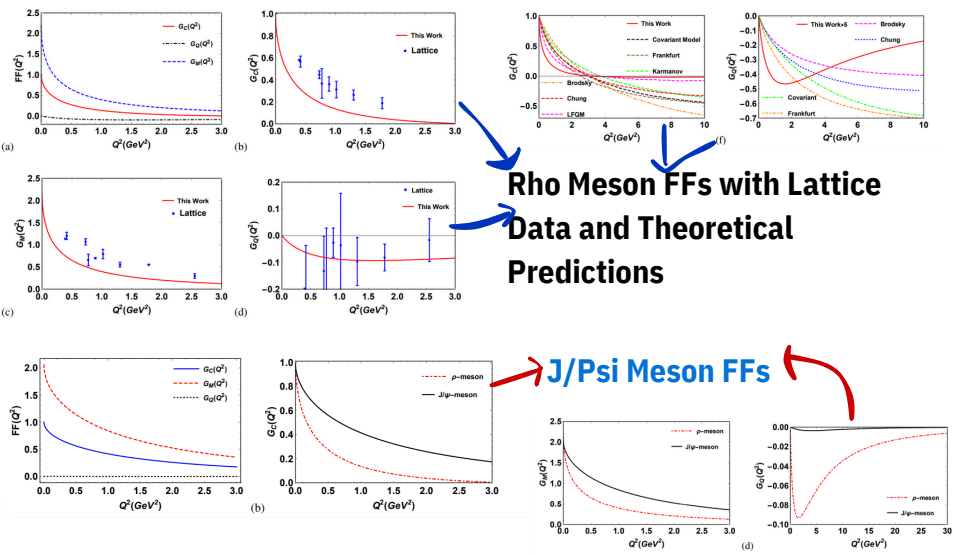
$$\int_{-1}^1 dx H_i(x, \xi, -\Delta_\perp^2) = 0. \quad (i = 4, 5)$$

Charge FF ————— $G_C(Q^2) = (1 + \frac{2}{3}\eta)F_1(Q^2) + \frac{2}{3}\eta F_2(Q^2) + \frac{2}{3}\eta(1 + \eta)F_3(Q^2),$

Magnetic FF ————— $G_M(Q^2) = F_2(Q^2),$

Quadrapole FF ————— $G_Q(Q^2) = F_1(Q^2) + F_2(Q^2) + (1 + \eta)F_3(Q^2).$

Spin-1 Form Factors



Rho Meson FFs with Lattice Data and Theoretical Predictions

J/Psi Meson FFs

Charge Radii, magnetic Moment and Quadrupole Moment

Charge Radii

$$\langle r_c^2 \rangle = \frac{-6}{G_C(0)} \left. \frac{\partial G_C(Q^2)}{\partial Q^2} \right|_{Q^2 \rightarrow 0}$$

Magnetic Moment

$$G_M(Q^2 = 0) = \mu_p$$

Quadrupole Moment

$$G_Q(Q^2 = 0) = Q_p$$

| | | $\sqrt{\langle r_c^2 \rangle}$ fm | μ_p | Q_p |
|--------------------|------------|-----------------------------------|---------|--------|
| $\rho(u\bar{d})$ | Our result | 0.95 | 2.19 | -0.023 |
| | Ref. [75] | 0.73 | 2.01 | -0.026 |
| | Ref. [78] | 0.82 | 2.07 | -0.045 |
| | Ref. [61] | 0.82 | 2.48 | -0.070 |
| | Ref. [74] | 0.56 | 0.75 | - |
| | Ref. [77] | 1.12 | 2.54 | - |
| $J/\psi(c\bar{c})$ | Our result | 0.69 | 2.05 | -0.006 |
| | Ref. [74] | 0.350 | 2.03 | - |
| | Ref. [75] | 0.24 | 2.12 | - |
| | Ref. [76] | 0.066 | 2.10 | - |

Helicity FFs

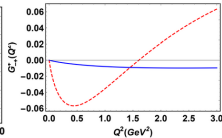
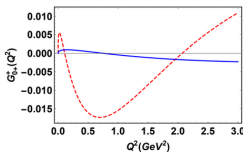
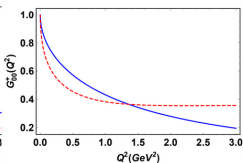
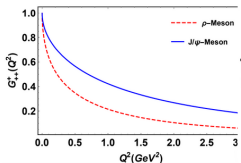
Futher, using $G_C(Q^2)$, $G_M(Q^2)$, and $G_Q(Q^2)$ form factors, one can define the conserving ($G_{++}^+(Q^2)$ and $G_{00}^+(Q^2)$) and non-conserving ($G_{-+}^+(Q^2)$ and $G_{0+}^+(Q^2)$) helicity matrix element as

$$G_{++}^+(Q^2) = \frac{1}{1+\eta} \left(G_C(Q^2) + \eta G_M(Q^2) + \frac{\eta}{3} G_Q(Q^2) \right),$$

$$G_{00}^+(Q^2) = \frac{1}{1+\eta} \left((1-\eta)G_C(Q^2) + 2\eta G_M(Q^2) - \frac{2\eta}{3}(1+2\eta)G_Q(Q^2) \right),$$

$$G_{0+}^+(Q^2) = -\frac{\sqrt{2}\eta}{1+\eta} \left(G_C(Q^2) - \frac{1}{2}(1-\eta)G_M(Q^2) + \frac{\eta}{3}G_Q(Q^2) \right),$$

$$G_{-+}^+(Q^2) = \frac{\eta}{1+\eta} \left(G_C(Q^2) - G_M(Q^2) - (1 + \frac{2\eta}{3})G_Q(Q^2) \right).$$



Structure Functions

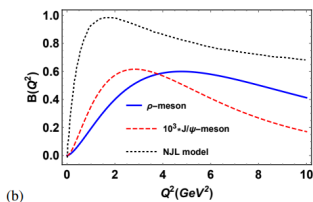
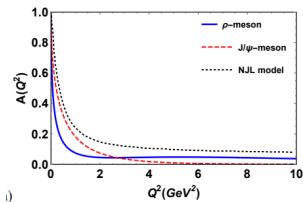
Rosenbluth cross section

$$\frac{d\sigma}{d(-Q^2)} = \frac{4\pi\alpha^2}{(-Q^2)^2} \left[\left(1 + \frac{(-Q^2)s}{(s - M_{\rho(J/\psi)}^2)^2} \right) A(Q^2) - \frac{M_{\rho(J/\psi)}^2(-Q^2)}{(s - M_{\rho(J/\psi)}^2)^2} B(Q^2) \right].$$

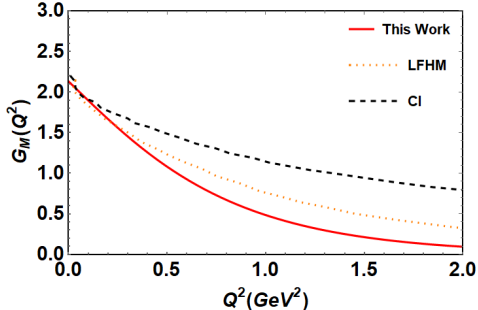
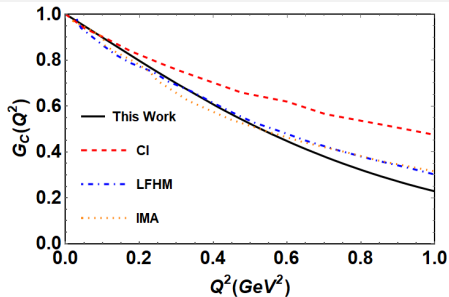
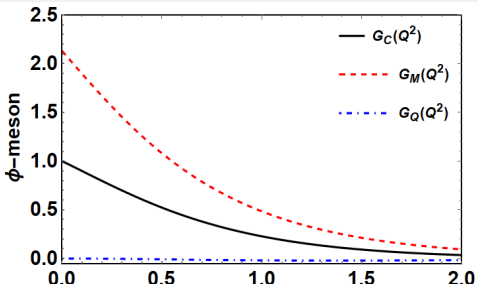
$$A(Q^2) = G_C^2(Q^2) + 2/3\eta G_M^2(Q^2) + 2(2/3)^2\eta^2 G_Q^2(Q^2),$$

$$B(Q^2) = \frac{4}{3}\eta(1 + \eta)G_M^2, \quad A(Q^2 = 0) = 1, \quad B(Q^2 = 0) = 0.$$

$$T_{20}(Q^2, \phi) = -\eta \frac{\sqrt{2} \frac{4}{3}\eta G_Q^2(Q^2) + 4G_Q(Q^2)G_C(Q^2) + (1/2 + (1 + \eta \tan^2 \frac{\phi}{2}))G_M^2(Q^2)}{3 A(Q^2) + B(Q^2) \tan^2 \frac{\phi}{2}}.$$



Phi Meson



| | | $\sqrt{\langle r_c^2 \rangle}$ fm | μ_p |
|------------------|-------------|-----------------------------------|---------|
| $\phi(s\bar{s})$ | This Work | 0.483 | 2.13 |
| | LFHM | 0.54 | 2.04 |
| | IMA | 0.60 | 2.18 |
| | CI | 0.47 | 2.09 |
| | Binosi 2019 | 0.52 | 2.08 |

Nuclear Medium Effect on DFs.

WHAAAA?!?!



Chiral SU(3) Quark Mean Field Model

- For medium modifications, we have adopted the chiral SU(3) quark mean field model.
 - The quarks are bound inside a hadron through confining potential and interact with each other via scalar fields.
 - Low energy properties: Chiral symmetry and its spontaneous breaking are incorporated in this model.
 - Broken- Scale invariance of QCD is also stimulated through the dilation field χ .
- The general effective Lagrangian density of CQMF model is expressed as

$$\mathcal{L}_{\text{eff}} = \mathcal{L}_{q0} + \mathcal{L}_{qm} + \mathcal{L}_{\Sigma\Sigma} + \mathcal{L}_{VV} + \mathcal{L}_{\chi SB} + \mathcal{L}_c.$$

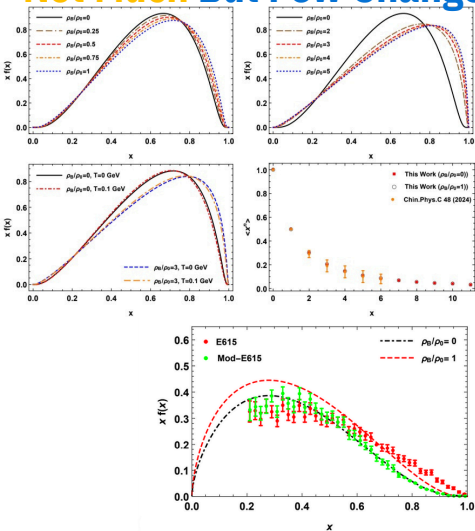
Chiral SU(3) Quark Mean Field Model

- $\mathcal{L}_{q0} = \bar{q} i\gamma^\mu \partial_\mu q$ is the kinetic term for quarks.
- \mathcal{L}_{qm} describes the interactions of constituent quarks with the scalar and vector mesons.
- The self-interactions of scalar mesons σ, ζ and δ and the dilaton field χ are described by the third term $\mathcal{L}_{\Sigma\Sigma}$.
- The fourth term \mathcal{L}_{VV} gives the self interactions of vector mesons ω and ρ .
- The term $\mathcal{L}_{\chi SB}$ representing the explicit symmetry breaking term.
- \mathcal{L}_c corresponds to the confinement of quarks inside the hadrons.

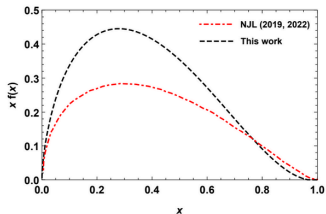
For More details- [S. Puhan, et.al, PRD, 110 \(2024\)](#).

Baryonic Density and Temperature effects on PDFs

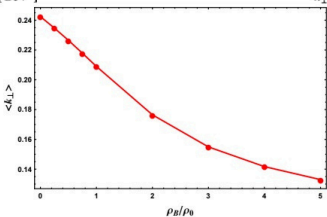
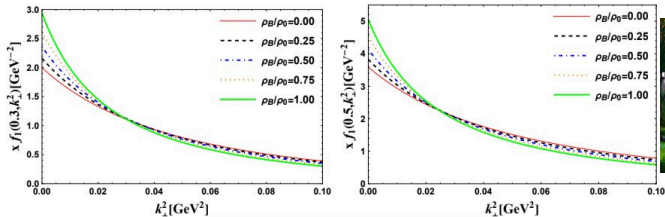
Not Much But Few Changes Occurring



Effect of Baryonic Density on Melin Moment of Pion



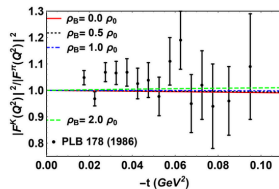
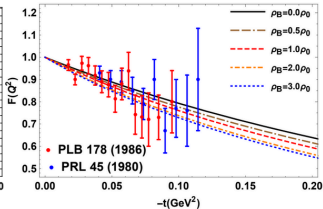
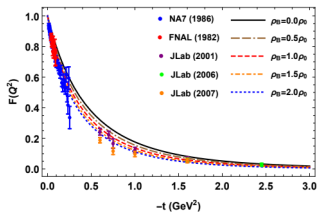
TMDs on Baryonic Density



**Effect of
Baryonic Density
on
Average
Transverse
Momenta of
Quark**

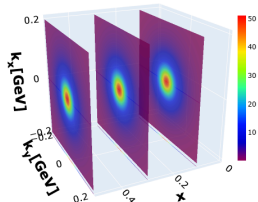
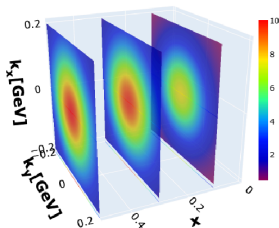
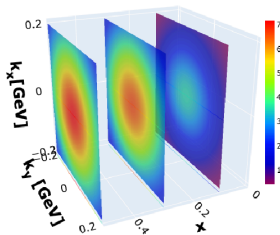
**Decrease in Average Momenta by 40
percentage**

Baryonic Density effect on FFs



| Baryonic density ratio (ρ_B/ρ_0) | LCQM (This work) | NJL Model [58] | LFQM [39] |
|--|---------------------------------------|---------------------------------------|---------------------------------------|
| | $\sqrt{\langle r_\pi^2 \rangle}$ (fm) | $\sqrt{\langle r_\pi^2 \rangle}$ (fm) | $\sqrt{\langle r_\pi^2 \rangle}$ (fm) |
| 0 | 0.523 | 0.629 | 0.654 |
| 0.5 | 0.553 | 0.664 | 0.776 |
| 1 | 0.585 | 0.694 | 0.947 |
| 1.5 | 0.614 | 0.714 | - |
| 2 | 0.638 | 0.730 | - |
| Exp. | 0.653(10) | - | - |
| Lat. | 0.648(2) | - | - |

Spin Densities in Medium



With Increase in Baryonic Density, the Spin Density becomes Concentrated around Zero





Dr. Harleen Dahiya



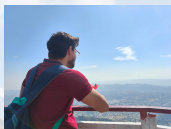
**Dr. Arvind Kumar
&
Dr. S Dutt**



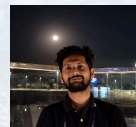
**Dr. Narinder Kumar
&
Dr. Nisha Dhiman**



Dr. Shubham Sharma



Mr. R. Pandey (JRF)



Mr. Asutosh Dwivedi



Mr. Ritwik (M. Sc)



Mr. Anurag (M.Sc)



Ms. Tanisha (M.Sc)



Mr. Abhishek (M.Sc)



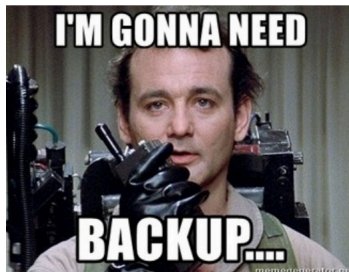
Mr. Hari (M.Sc)

Thank You



Backup Slides

Backup Slides



Backup Slides

Sorry, NO Backup Slides